

Design, Synthesis, Biological Evaluation, and Structure–Activity Relationships of Substituted Phenyl 4-(2-Oxoimidazolidin-1-yl)-benzenesulfonates as New Tubulin Inhibitors Mimicking Combretastatin A-4

Sébastien Fortin,^{*,†,‡} Lianhu Wei,[§] Emmanuel Moreau,^{||} Jacques Lacroix,[†] Marie-France Côté,[†] Éric Petitclerc,^{†,∞} Lakshmi P. Kotra,^{§,⊥} and René C.-Gaudreault^{*,†,‡,¶}

[†]Unité des Biotechnologies et de Bioingénierie, Centre de Recherche, C.H.U.Q., Hôpital Saint-François d'Assise, Québec, Québec, G1L 3L5, Canada

[‡]Faculté de Pharmacie, Université Laval, Pavillon Vandry, Québec, Québec, G1V 0A6, Canada

[§]Center for Molecular Design and Preformulations, Toronto General Research Institute, University Health Network, Toronto, Ontario, M5G 1L7, Canada

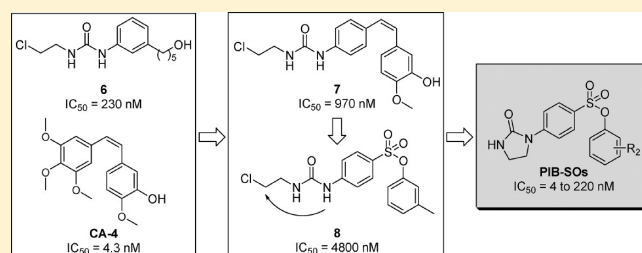
^{||}Clermont 1, Université d'Auvergne, Inserm, U 990, F-63000 Clermont-Ferrand, France

[⊥]Department of Pharmaceutical Sciences, Leslie Dan Faculty of Pharmacy, University of Toronto, Toronto, Ontario, M5S 3M2, Canada

[∞]Faculté de Médecine, Université Laval, Pavillon Vandry, Québec, Québec, G1V 0A6, Canada

S Supporting Information

ABSTRACT: Sixty-one phenyl 4-(2-oxoimidazolidin-1-yl)-benzenesulfonates (PIB-SOs) and 13 of their tetrahydro-2-oxopyrimidin-1(2H)-yl analogues (PPB-SOs) were prepared and biologically evaluated. The antiproliferative activities of PIB-SOs on 16 cancer cell lines are in the nanomolar range and unaffected in cancer cells resistant to colchicine, paclitaxel, and vinblastine or overexpressing the P-glycoprotein. None of the PPB-SOs exhibit significant antiproliferative activity. PIB-SOs block the cell cycle progression in the G₂/M phase and bind to the colchicine-binding site on β -tubulin leading to cytoskeleton disruption and cell death. Chick chorioallantoic membrane tumor assays show that compounds **36**, **44**, and **45** efficiently block angiogenesis and tumor growth at least at similar levels as combretastatin A-4 (CA-4) and exhibit low to very low toxicity on the chick embryos. PIB-SOs were subjected to CoMFA and CoMSIA analyses to establish quantitative structure–activity relationships.



INTRODUCTION

Microtubules are key components of the cytoskeleton and are involved in a wide range of cellular functions, notably cell division where they are responsible for mitotic spindle formation and proper chromosomal separation.¹ Consequently, microtubules have been for the past decades important targets for the design and the development of several potent natural and synthetic anticancer drugs² such as paclitaxel,³ epothilone A,⁴ vinblastine,⁵ and combretastatin A-4⁶ (**1**, CA-4), molecules that are of utmost importance in the management of cancers such as ovarian, breast, and prostate cancers.^{7,8} However, the efficacy and the clinical usefulness of currently available antimicrotubules is impeded by the occurrence of chemoresistance, systemic toxicity, and poor biopharmaceutical properties.^{9,10} Therefore, the search for new antimicrotubule agents exhibiting improved biopharmaceutical profiles and pharmacodynamics is the focus of numerous academic and industrial teams.¹¹

In the past decades, ligands to the colchicine-binding site (CBS) were extensively studied and many interesting compounds

were identified and tested. To that end, CA-4 isolated from the bark of *Combretum caffrum*¹² was shown to exhibit potent antiangiogenic and antitumoral activities. However, poor solubility of the drug impinged its clinical development and required the preparation of more soluble derivatives such as CA-4 phosphate sodium salt¹³ (**2**) and the amino acid hydrochloride salt¹⁴ (**3**). These molecules represent promising drugs in various clinical settings, showing potent activities to disrupt vasculature and to reduce significantly the tumoral blood flow.¹⁵ Unfortunately, CA-4, **2**, and **3** exhibit many deleterious effects such as hypertension, hypotension, tachycardia, tumor pain, and lymphopenia.¹⁶ In addition, the activity of CA-4, **2**, and **3** is hampered by a short biological half-life^{17,18} and isomerization of their active *cis*-stilbene conformation into the corresponding inactive *trans* analogues.^{13,19} To overcome the problem, the ethenyl bridge

Received: February 16, 2011

Published: May 23, 2011

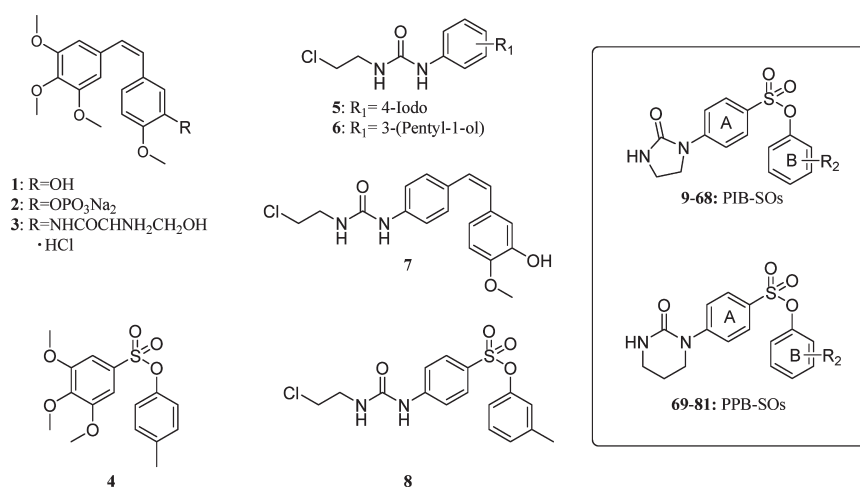


Figure 1. Structures of CA-4 and 2–81.

of the stilbene moiety was converted into more biologically stable molecules utilizing polar groups such as carbonyl (e.g., phenstatin),²⁰ arylthioindole,²¹ oxazole, triazole, and thiophene bioisosteres.²² In that context, Gweltaney et al. have successfully converted the ethenyl group of CA-4 into the more stable and more polar sulfonate group²³ (4).

N-Phenyl-*N'*-(2-chloroethyl)urea (CEU) is another class of antimicrotubule agent characterized by its unique ability to acylate Glu198 of β -tubulin, an amino acid located in a pocket adjacent to the C-BS. The acylation of Glu198 leads to microtubule depolymerization, hypoacetylation of Lys40 on α -tubulin, cytoskeleton disruption, and anoikis.^{24,25} CEU analogues such as 1-(2-chloroethyl)-3-(4-iodophenyl)urea (5)^{26–28} or 1-(2-chloroethyl)-3-(3-(5-hydroxypentyl)phenyl)urea (6)^{29–31} inhibit angiogenesis and tumor growth in three distinct animal models.²⁵ The biodistribution of CEU analogues to organs of the gastrointestinal tract suggests that they might be promising new drugs for the treatment of colorectal cancers.^{32,33} Several CEU subsets were also found to be devoid of antimicrotubule affinity and to bind covalently to proteins such as thioredoxin isoform 1,^{34–36} prohibitin 1,³⁷ and the mitochondrial voltage-dependent anion channel 1.³⁸

DESIGN OF SUBSTITUTED PHENYL (2-OXOIMIDAZOLIDIN-1-YL)BENZENESULFONATES

Computational experiments conducted on antimicrotubule CEU analogues led to the hypothesis that the *N*-phenyl-*N'*-(2-chloroethyl)urea pharmacophore moiety of CEU might be a bioisosteric equivalent to the trimethoxyphenyl ring of CA-4 and several other drugs binding to the C-BS.^{39,40} This hypothesis was confirmed by the synthesis and biological evaluation of molecular hybrids where the trimethoxyphenyl moiety of CA-4 was replaced by the pharmacophore moiety of CEU to give compounds such as 1-(4-(3-hydroxy-4-methoxystyryl)phenyl)-3-(2-chloroethyl)urea (7).⁴¹ Several of these molecular hybrids exhibited antiproliferative activity through the acylation of Glu198 as observed with the original CEU. Subsequently, we initiated the development of new CEU analogues incorporating the molecular scaffold of CA-4 to enhance efficacy, stability, and polarity. We prepared new molecular hybrids based on the conversion of the trimethoxyphenyl ring of compound 4 into an *N*-phenyl-*N'*-(2-chloroethyl)urea moiety to generate several CEU-sulfonate

analogues (8). A number of 8 derivatives exhibited cytotoxic activity at the micromolar level on several tumor cell lines and generally blocked the cell cycle progression in the G₂/M phase. We previously showed that the cyclization of the 2-chloroethylurea moiety of CEU into 4,5-dihydrooxazol-2-amine derivatives improved the cytotoxic activity of CEU.^{34,36,42} On the basis of these results, we hypothesized that the cyclization of the *N*-phenyl-*N'*-(2-chloroethyl)urea moiety of 8 might also be beneficial to the antiproliferative activity.

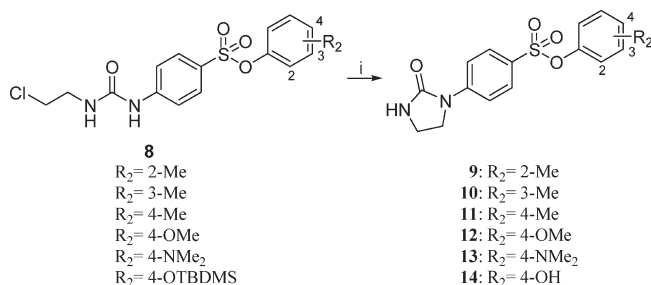
In this study, we described the preparation and the evaluation of new phenyl 4-(2-oxoimidazolidin-1-yl)benzenesulfonate derivatives (PIB-SOs) as antiproliferative agents targeting the C-BS. We assessed the effect of the nature and the position of the substituents on the aromatic ring B (PIB-SOs 9–68) on the antiproliferative activity, on the binding to the C-BS, and on the antineoplastic and toxic activities on human cancer cells grafted onto the chick chorioallantoic membrane tumor (CAM) assays. Thirteen of the most potent PIB-SO derivatives were used to evaluate the effect on the aforementioned parameters of enlarging the imidazolidin-2-one ring of PIB-SO into a tetrahydropyrimidin-2(1*H*)-one ring (PPB-SOs 69–81) (Figure 1).

RESULTS

Chemistry. Initially, 8 derivatives were prepared as follows. 4-Nitrodiphenylsulfonates were obtained by nucleophilic addition of the appropriate phenol to 4-nitrophenylsulfonyl chloride followed by the reduction of the nitro group into its aniline. The relevant anilines were then added to 2-chloroethyl isocyanate to yield the corresponding 8 derivatives. Finally, PIB-SOs 9–14 were prepared from the catalytic cyclization of the CEU sulfonates in the presence of KF adsorbed on Al₂O₃ (4:6) in refluxing acetonitrile (Scheme 1).

The aforementioned preparation of 8 derivatives was a long and tedious process. Therefore, we used an easier and more efficient approach for the synthesis of PIB-SOs and PPB-SOs 9–81 (Scheme 2)^{43,44} based on the nucleophilic addition of aniline to either 2-chloroethyl isocyanate or 3-chloropropyl isocyanate in methylene chloride at 25 °C followed by cyclization into the corresponding 1-phenylimidazolidin-2-one (84) or tetrahydro-3-phenylpyrimidin-2(1*H*)-one (85) using sodium hydride in THF at 25 °C. Compound 84 was also prepared using triphosgene,

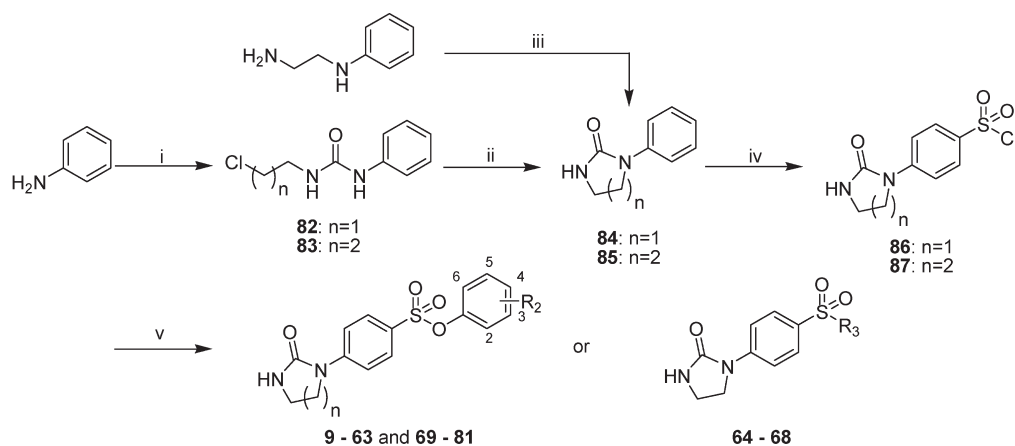
N-phenylethylenediamine, and triethylamine in anhydrous tetrahydrofuran at 0 °C. 4-(2-Oxoimidazolidin-1-yl)benzene-1-sulfonyl chloride (**86**) and 4-(tetrahydro-2-oxypyrimidin-1(2*H*)-yl)benzene-1-sulfonyl chloride (**87**) were obtained by chlorosulfonation of

Scheme 1^a

^a Reagents and conditions: (i) $\text{Al}_2\text{O}_3/\text{KF}$, CH_3CN .

84 and **85** by chlorosulfonic acid in carbon tetrachloride at 0 °C. Compounds **9**–**81** were synthesized by nucleophilic addition of an appropriate phenol on either compound **86** or **87** in the presence of triethylamine in methylene chloride at 25 °C. Aniline **40**, **51**, and **63** were obtained by the reduction of the nitro group on **39**, **50**, and **62** under hydrogen atmosphere in the presence of palladium on charcoal in ethanol. Phenol **14** was obtained by deprotection of the *tert*-butyldimethylsilyl intermediate **58** in the presence of tributylammonium fluoride in THF.

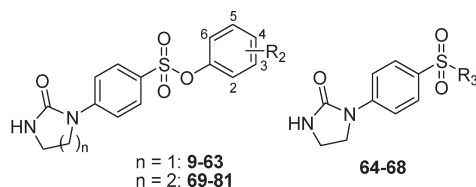
Evaluation of the Antiproliferative Activity. The antiproliferative activity of PIB-SO and PPB-SO derivatives was assessed on three human cancer cell lines, namely, HT-29 colon carcinoma, M21 skin melanoma, and MCF7 breast carcinoma cells. These cell lines were selected, as they are good representatives of tumor cells originating from the three embryonic germ layers. Cell growth inhibition was assessed according to the NCI/NIH Developmental Therapeutics Program.⁴⁵ The results are summarized in Table 1 and expressed as the concentration of drug inhibiting cell growth by 50% (IC_{50}).

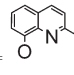
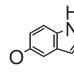
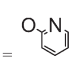
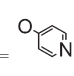
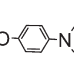
Scheme 2^a

9: $n = 1, R_2 = 2\text{-Me}$	37: $n = 1, R_2 = 3\text{-F}$	64: $R_3 =$
10: $n = 1, R_2 = 3\text{-Me}$	38: $n = 1, R_2 = 3\text{-I}$	65: $R_3 =$
11: $n = 1, R_2 = 4\text{-Me}$	39: $n = 1, R_2 = 3\text{-NO}_2$	66: $R_3 =$
12: $n = 1, R_2 = 4\text{-OMe}$	40: $n = 1, R_2 = 3\text{-NH}_2$	67: $R_3 =$
13: $n = 1, R_2 = 4\text{-NMe}_2$	41: $n = 1, R_2 = 3\text{-Me, 5-Me}$	68: $R_3 =$
14: $n = 1, R_2 = 4\text{-OH}$	42: $n = 1, R_2 = 3\text{-Me, 4-Me, 5-Me}$	69: $n = 2, R_2 = 2\text{-Me}$
15: $n = 1, R_2 = \text{H}$	43: $n = 1, R_2 = 3\text{-OMe, 4-OMe}$	70: $n = 2, R_2 = 2\text{-Et}$
16: $n = 1, R_2 = 2\text{-Et}$	44: $n = 1, R_2 = 3\text{-OMe, 5-OMe}$	71: $n = 2, R_2 = 2\text{-Prop}$
17: $n = 1, R_2 = 2\text{-Prop}$	45: $n = 1, R_2 = 3\text{-OMe, 4-OMe, 5-OMe}$	72: $n = 2, R_2 = 2\text{-Me, 4-Me}$
18: $n = 1, R_2 = 2\text{-OMe}$	46: $n = 1, R_2 = 3\text{-Cl, 5-Cl}$	73: $n = 2, R_2 = 2\text{-Cl, 4-Cl, 5-Cl}$
19: $n = 1, R_2 = 2\text{-OEt}$	47: $n = 1, R_2 = 3\text{-F, 4-F}$	74: $n = 2, R_2 = 2\text{-Cl, 4-Cl, 6-Cl}$
20: $n = 1, R_2 = 2\text{-Cl}$	48: $n = 1, R_2 = 3\text{-F, 5-F}$	75: $n = 2, R_2 = 3\text{-Me}$
21: $n = 1, R_2 = 2\text{-F}$	49: $n = 1, R_2 = 3\text{-F, 4-F, 5-F}$	76: $n = 2, R_2 = 3\text{-OMe}$
22: $n = 1, R_2 = 2\text{-I}$	50: $n = 1, R_2 = 3\text{-Me, 4-NO}_2$	77: $n = 2, R_2 = 3\text{-F}$
23: $n = 1, R_2 = 2\text{-NO}_2$	51: $n = 1, R_2 = 3\text{-Me, 4-NH}_2$	78: $n = 2, R_2 = 3\text{-OMe, 4-OMe, 5-OMe}$
24: $n = 1, R_2 = 2\text{-Me, 3-Me}$	52: $n = 1, R_2 = 4\text{-Et}$	79: $n = 2, R_2 = 4\text{-Me}$
25: $n = 1, R_2 = 2\text{-Me, 4-Me}$	53: $n = 1, R_2 = 4\text{-Prop}$	80: $n = 2, R_2 = 4\text{-Cl}$
26: $n = 1, R_2 = 2\text{-Me, 5-Me}$	54: $n = 1, R_2 = 4\text{-secBut}$	81: $n = 2, R_2 = 4\text{-F}$
27: $n = 1, R_2 = 2\text{-Me, 4-Me, 5-Me}$	55: $n = 1, R_2 = 4\text{-OEt}$	
28: $n = 1, R_2 = 2\text{-Cl, 4-Cl, 5-Cl}$	56: $n = 1, R_2 = 4\text{-OProp}$	
29: $n = 1, R_2 = 2\text{-Cl, 4-Cl, 6-Cl}$	57: $n = 1, R_2 = 4\text{-OBut}$	
30: $n = 1, R_2 = 2\text{-F, 4-F}$	58: $n = 1, R_2 = 4\text{-OTBDMS}$	
31: $n = 1, R_2 = 2\text{-F, 6-F}$	59: $n = 1, R_2 = 4\text{-Cl}$	
32: $n = 1, R_2 = 2\text{-F, 3-F, 4-F, 5-F, 6-F}$	60: $n = 1, R_2 = 4\text{-F}$	
33: $n = 1, R_2 = 3\text{-Prop}$	61: $n = 1, R_2 = 4\text{-I}$	
34: $n = 1, R_2 = 3\text{-OMe}$	62: $n = 1, R_2 = 4\text{-NO}_2$	
35: $n = 1, R_2 = 3\text{-OEt}$	63: $n = 1, R_2 = 4\text{-NH}_2$	
36: $n = 1, R_2 = 3\text{-Cl}$		

^a Reagents and conditions: (i) 2-chloroethyl isocyanate or 3-chloropropyl isocyanate, DCM; (ii) NaH, THF; (iii) triphosgene, TEA, THF; (iv) ClSO_3H , CCl_4 ; (v) relevant phenol, triethylamine, DCM; (vi) H_2 , Pd/C 10%, EtOH; (vii) TBAF, THF.

Table 1. Evaluation of the Antiproliferative Activity of PIB-SOs, PPB-SOs, CA-4, and Compound 6 on HT-29, M21, and MCF7 Cells



Compd	n ^a	R ₂ or R ₃	IC ₅₀ (nM) ^b			Compd	n ^a	R ₂ or R ₃	IC ₅₀ (nM) ^b		
			HT-29	M21	MCF7				HT-29	M21	MCF7
9	1	R ₂ = 2-Me	33	26	30	51	1	R ₂ = 3-Me, 4-NH ₂	670	360	600
10	1	R ₂ = 3-Me	76	54	57	52	1	R ₂ = 4-Et	150	120	190
11	1	R ₂ = 4-Me	120	93	150	53	1	R ₂ = 4-Prop	77	59	110
12	1	R ₂ = 4-OMe	130	98	160	54	1	R ₂ = 4-secBut	780	830	920
13	1	R ₂ = 4-NMe ₂	430	350	500	55	1	R ₂ = 4-OEt	44	39	56
14	1	R ₂ = 4-OH	> 1 000	> 1 000	> 1 000	56	1	R ₂ = 4-OProp	110	96	140
15	1	R ₂ = H	> 1 000	> 1 000	> 1 000	57	1	R ₂ = 4-OBut	540	530	890
16	1	R ₂ = 2-Et	61	52	87	58	1	R ₂ = 4-OTBDMS	> 1 000	> 1 000	> 1 000
17	1	R ₂ = 2-Prop	76	61	69	59	1	R ₂ = 4-Cl	87	58	88
18	1	R ₂ = 2-OMe	180	130	220	60	1	R ₂ = 4-F	120	89	170
19	1	R ₂ = 2-OEt	40	24	83	61	1	R ₂ = 4-I	150	110	210
20	1	R ₂ = 2-Cl	66	45	73	62	1	R ₂ = 4-NO ₂	> 1 000	570	> 1 000
21	1	R ₂ = 2-F	51	34	61	63	1	R ₂ = 4-NH ₂	> 1 000	920	> 1 000
22	1	R ₂ = 2-I	55	40	71	64	-		180	130	330
23	1	R ₂ = 2-NO ₂	190	150	270	65	-		70	65	100
24	1	R ₂ = 2-Me, 3-Me	31	17	50	66	-		480	290	770
25	1	R ₂ = 2-Me, 4-Me	51	39	50	67	-		> 1 000	> 1 000	> 1 000
26	1	R ₂ = 2-Me, 5-Me	10	8.5	14	68	-		> 1 000	> 1 000	> 1 000
27	1	R ₂ = 2-Me, 4-Me, 5-Me	42	41	66	69	2	R ₂ = 2-Me	> 1 000	> 1 000	> 1 000
28	1	R ₂ = 2-Cl, 4-Cl, 5-Cl	30	31	30	70	2	R ₂ = 2-Et	> 1 000	> 1 000	> 1 000
29	1	R ₂ = 2-Cl, 4-Cl, 6-Cl	110	120	170	71	2	R ₂ = 2-Prop	> 1 000	> 1 000	> 1 000
30	1	R ₂ = 2-F, 4-F	41	35	55	72	2	R ₂ = 2-Me, 4-Me	> 1 000	> 1 000	> 1 000
31	1	R ₂ = 2-F, 6-F	29	15	32	73	2	R ₂ = 2-Cl, 4-Cl, 5-Cl	> 1 000	> 1 000	> 1 000
32	1	R ₂ = 2-F, 3-F, 4-F, 5-F, 6-F	340	220	320	74	2	R ₂ = 2-Cl, 4-Cl, 6-Cl	> 1 000	> 1 000	> 1 000
33	1	R ₂ = 3-Prop	34	27	51	75	2	R ₂ = 3-Me	> 1 000	> 1 000	> 1 000
34	1	R ₂ = 3-OMe	29	24	34	76	2	R ₂ = 3-OMe	> 1 000	> 1 000	> 1 000
35	1	R ₂ = 3-OEt	18	12	19	77	2	R ₂ = 3-F	> 1 000	> 1 000	> 1 000
36	1	R ₂ = 3-Cl	15	9.2	13	78	2	R ₂ = 3-OMe, 4-OMe, 5-OMe	490	240	730
37	1	R ₂ = 3-F	42	31	54	79	2	R ₂ = 4-Me	720	> 1 000	> 1 000
38	1	R ₂ = 3-I	11	10	18	80	2	R ₂ = 4-Cl	> 1 000	> 1 000	> 1 000
39	1	R ₂ = 3-NO ₂	100	48	60	81	2	R ₂ = 4-F	> 1 000	> 1 000	> 1 000
40	1	R ₂ = 3-NH ₂	> 1 000	170	270	6	-		150	230	420
41	1	R ₂ = 3-Me, 5-Me	32	16	47	6	-		150	230	420
42	1	R ₂ = 3-Me, 4-Me, 5-Me	34	15	49	CA-4	-		61	4.3	5.6
43	1	R ₂ = 3-OMe, 4-OMe	67	45	88						
44	1	R ₂ = 3-OMe, 5-OMe	8.0	4.3	10						
45	1	R ₂ = 3-OMe, 4-OMe, 5-OMe	4.0	4.0	5.0						
46	1	R ₂ = 3-Cl, 5-Cl	10	8.2	18						
47	1	R ₂ = 3-F, 4-F	75	47	100						
48	1	R ₂ = 3-F, 5-F	36	15	47						
49	1	R ₂ = 3-F, 4-F, 5-F	73	43	91						
50	1	R ₂ = 3-Me, 4-NO ₂	140	100	180						

^aThe dash (–) indicates “not applicable”. ^bIC₅₀ is expressed as the concentration of drug inhibiting cell growth by 50%.

Table 2. Effects of the Most Potent PIB-SOs, CA-4, and Compound 6 on Cell Cycle Progression, Cytoskeleton Integrity, and Results of a Competition Assay with EBI

Compd	R ₂ , R ₃	Cell cycle progression ^a			EBI competition assay ^{b,c}	Cytoskeleton integrity ^d
		G ₀ /G ₁ (%)	S (%)	G ₂ /M (%)		
9	R ₂ = 2-Me	11	15	74	++	
10	R ₂ = 3-Me	1	0	99	+++	
11	R ₂ = 4-Me	32	13	55	-	
12	R ₂ = 4-OMe	0	5	95	+	
16	R ₂ = 2-Et	0	0	100	+++	
17	R ₂ = 2-Prop	0	0	100	+	
19	R ₂ = 2-OEt	1	19	80	+++	
20	R ₂ = 2-Cl	2	15	83	+++	
21	R ₂ = 2-F	18	34	48	++	
22	R ₂ = 2-I	4	25	71	+++	
24	R ₂ = 2-Me, 3-Me	5	32	63	+++	
25	R ₂ = 2-Me, 4-Me	0	0	100	+	
26	R ₂ = 2-Me, 5-Me	3	20	77	+++	
27	R ₂ = 2-Me, 4-Me, 5-Me	1	20	79	++	
28	R ₂ = 2-Cl, 4-Cl, 5-Cl	1	0	99	+++	

Table 2. Continued


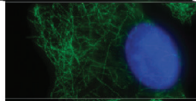

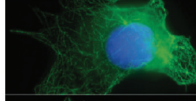
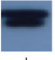
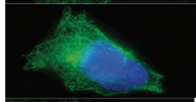

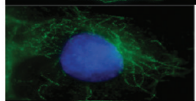

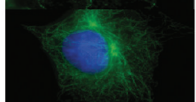

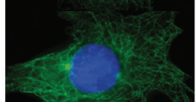

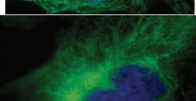

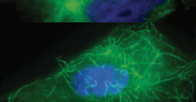

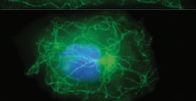

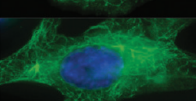

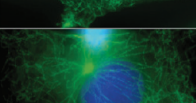
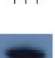
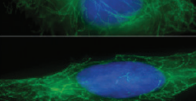

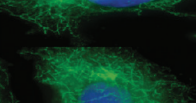
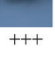
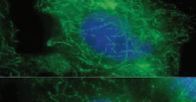

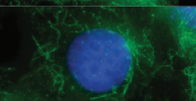

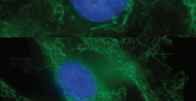

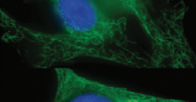

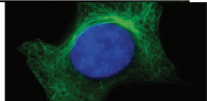

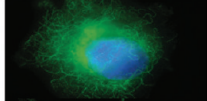

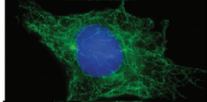

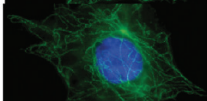

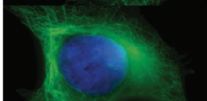

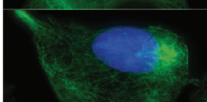
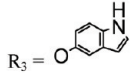

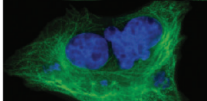
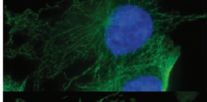
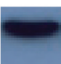
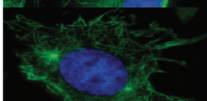

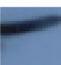
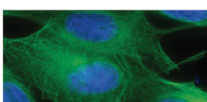
Compd	R ₂ , R ₃	Cell cycle progression ^a			EBI competition assay ^{b,c}	Cytoskeleton integrity ^d
		G ₀ /G ₁ (%)	S (%)	G ₂ /M (%)		
30	R ₂ = 2-F, 4-F	2	26	72	 ++	
31	R ₂ = 2-F, 6-F	5	33	62	 +++	
33	R ₂ = 3-Prop	2	25	73	 +	
34	R ₂ = 3-OMe	1	1	98	 +++	
35	R ₂ = 3-OEt	2	20	78	 +++	
36	R ₂ = 3-Cl	2	19	79	 +++	
37	R ₂ = 3-F	7	9	84	 ++	
38	R ₂ = 3-I	2	21	77	 +++	
39	R ₂ = 3-NO ₂	56	13	31	 +++	
41	R ₂ = 3-Me, 5-Me	7	26	67	 +++	
42	R ₂ = 3-Me, 4-Me, 5-Me	0	0	99	 +++	
43	R ₂ = 3-OMe, 4-OMe	1	19	80	 +++	
44	R ₂ = 3-OMe, 5-OMe	1	24	75	 +++	
45	R ₂ = 3-OMe, 4-OMe, 5-OMe	1	1	98	 +++	
46	R ₂ = 3-Cl, 5-Cl	1	20	79	 +++	
47	R ₂ = 3-F, 4-F	2	26	72	 +	
48	R ₂ = 3-F, 5-F	12	29	59	 +++	

Table 2. Continued

Compd	R ₂ , R ₃	Cell cycle progression ^a			EBI competition assay ^{b,c}	Cytoskeleton integrity ^d
		G ₀ /G ₁ (%)	S (%)	G ₂ /M (%)		
49	R ₂ = 3-F, 4-F, 5-F	4	31	65	 +	
53	R ₂ = 4-Prop	1	18	81	 +	
55	R ₂ = 4-OEt	2	23	75	 +	
56	R ₂ = 4-OProp	0	6	94	 +	
59	R ₂ = 4-Cl	0	0	100	 +++	
60	R ₂ = 4-F	51	21	28	 ++	
65	R ₃ = 	19	17	64	 +++	
6		1	11	88	N/A	
CA-4		2	0	98	 +++	
EBI		N/A	N/A	N/A	 N/A	N/A
DMSO		61	30	9	 N/A	

^a For cell cycle progression, M21 cells were incubated in presence of PIB-SOs at 5 times their respective IC₅₀ for 24 h. ^b For competition assay with EBI, MDA-MB-231 cells were incubated in the presence of PIB-SOs at 1000 times their respective IC₅₀ for 2 h and afterward in the presence of 100 μM EBI for 1.5 h. ^c Inhibition coding: +++, strong inhibition; ++, significant inhibition; +, weak inhibition; -, no inhibition; N/A, not applicable. ^d M21 cells were treated for 16 h with the drug at 5 times their respective IC₅₀, and cellular microtubule structures were visualized using indirect immunofluorescence using an anti-β-tubulin monoclonal antibody.

Mechanism of Action. CA-4 and compounds 2–7 are known C-BS antagonists, disrupting the polymerization of tubulin heterodimers, inhibiting cell cycle progression in the G₂/M phase, and leading to anoikis. Therefore, we have conducted experiments to identify the mechanism involved in the cytotoxic activity of PIB-SOs in relation to their expected binding to the C-BS on β-tubulin. The evaluation was conducted using compounds 9–12, 16, 17, 19–22, 24–28, 30, 31, 33–39, 41–49, 53, 55, 56, 59, 60, and 65 that were exhibiting IC₅₀ lower than 100 nM in M21 tumor cells. We first assessed their effects on cell cycle progression. Table 2 shows the percentage of M21 cells in G₀/G₁, S, and G₂/M phases after treatment with the selected PIB-SOs together with CA-4 and compound 6 at 5 times their respective IC₅₀.

Afterward, we assessed the binding of these compounds to the colchicine-binding site. To that end, we developed a quick and simple detection procedure based on the competition between the bishioalkylation of Cys239 and Cys354 by *N,N'*-ethylenebis(iodoacetamide) (EBI) and drugs binding to the C-BS to assess the ability of anti-C-BS agents to occupy that binding site.⁴⁶ Briefly, the β-tubulin adduct formed by the covalent binding of EBI on Cys239 and Cys354 is easily detectable by Western blot as an immunoreacting band of β-tubulin migrating faster than the native β-tubulin. The occupancy of the C-BS by relevant antimicrotubule inhibitors inhibits the formation of the EBI/β-tubulin adduct, resulting in an assay that allows the easy and inexpensive screening of new molecules targeting the C-BS. Table 2 shows

Table 3. Antiproliferative Activity of Compounds 12, 26, 31, 35, 36, 38, 44–46, 60, Colchicine, Paclitaxel, and Vinblastine on CHO, K562, L1210, P388D1, B16F0, DU-145, HT-1080, MDA-MB-231, SKOV3, and CEM Cells

compd	IC ₅₀ (nM) ^d									
	CHO	K562	L1210	P388D1	B16F0	DU 145	HT-1080	MDA-MB-231	SKOV3	CEM
12	240	240	250	260	510	650	240	760	320	250
26	18	18	21	19	49	57	24	69	29	19
31	73	65	67	76	91	170	65	100	72	68
35	32	18	19	20	65	72	34	55	42	20
36	18	16	17	19	46	58	19	45	22	17
38	17	14	19	18	30	57	19	48	23	17
44	7.3	7.5	6.4	7.8	25	25	8.2	14	6.8	7.1
45	7.4	2.5	5.4	2.7	9.2	8.5	5.9	9.4	6.1	7.1
46	17	7.2	9.6	7.4	41	66	18	26	16	16
60	230	180	140	240	250	550	190	360	210	200
Col ^a	220	6.8	6.9	28	13	10	1.1	2.9	2.1	7.9
Pac ^b	170	0.71	0.40	35	28	1.3	0.15	9.1	2.6	0.27
Vbl ^c	17	0.36	0.16	1.8	0.099	0.063	0.099	0.12	0.039	0.38

^a Col, colchicine. ^b Pac, paclitaxel. ^c Vbl, vinblastine. ^d IC₅₀: concentration of drug inhibiting cell growth by 50%.

Table 4. Antiproliferative Activity of Compounds 12, 26, 31, 35, 36, 38, 44–46, 60, Colchicine, Paclitaxel, and Vinblastine on Chemoresistant TAX 5-6, CHO-VV 3-2, and CEM-VLB Cells

compd	IC ₅₀ (nM) ^d	ratio resistant/wild-type	IC ₅₀ (nM) ^d	ratio resistant/wild-type	IC ₅₀ (nM) ^d	ratio resistant/wild-type
	CHO-TAX 5-6 ^e	CHO-TAX 5-6/CHO	CHO-VV 3-2 ^f	CHO-VV 3-2/CHO	CEM-VLB ^g	CEM-VLB/CEM
12	200	0.83	250	1.0	320	1.3
26	14	0.78	21	1.2	23	1.2
31	38	0.52	74	1.0	87	1.3
35	12	0.38	39	1.2	32	1.6
36	9.3	0.52	20	1.1	20	1.2
38	8.9	0.52	20	1.2	18	1.1
44	5.2	0.71	15	2.1	9.2	1.3
45	3	0.41	8.2	1.1	9.5	1.3
46	6.1	0.36	20	1.2	19	1.2
60	86	0.37	260	1.1	270	1.4
Col ^a	140	0.64	620	2.8	360	46
Pac ^b	520	3.1	140	0.82	3340	12370
Vbl ^c	6.9	0.41	66	3.9	600	1579

^a Col, colchicine. ^b Pac, paclitaxel. ^c Vbl, vinblastine. ^d IC₅₀: concentration of drug inhibiting cell growth by 50%. ^e Paclitaxel-resistant CHO-TAX 5-6 cells.

^f Colchicine- and vinblastine-resistant CHO-VV 3-2 cells. ^g Multidrug-resistant leukemia CEM-VLB cells.

the results obtained from the competition between EBI at 100 μ M and PIB-SOs 9–12, 16, 17, 19–22, 24–28, 30, 31, 33–39, 41–49, 53, 55, 56, 59, 60, and 65 at 1000 times their respective IC₅₀ on MDA-MB-231 cells. Finally, the effect of PIB-SOs on the cytoskeleton was also visualized using a fluorescent anti- β -tubulin antibody and immunofluorescence techniques (Table 2).

Antiproliferative Activity of PIB-SOs on Chemoresistant and Wild-Type Cancer Cells. The antiproliferative activity of compounds 12, 26, 31, 35, 36, 38, 44–46, and 60 was assessed on 10 wild-type cancer and three chemoresistant cell lines (Tables 3 and 4). Wild-type cancer cell lines were Chinese hamster ovary CHO, human chronic myelogenous leukemia K562, murine lymphocytotic leukemia L1210, murine macrophages P388D1, murine melanoma B16F0, human prostate carcinoma DU 145, human fibrosarcoma HT-1080, human breast adenocarcinoma MDA-MB-231, human ovarian SKOV3, and T cell leukemia

CEM cells. Chemoresistant cancer cells were paclitaxel-resistant CHO-TAX 5-6⁴⁷ colchicine- and vinblastine-resistant CHO-VV 3-2,⁴⁸ and multidrug-resistant leukemia CEM-VLB^{49,50} cells. Colchicine,⁵¹ paclitaxel, and vinblastine were used as positive controls. The concentration of drug inhibiting cell growth by 50% is expressed as the IC₅₀. Cell growth inhibition was assessed according to the NCI/NIH Developmental Therapeutics Program.⁴⁵

CAM Assay. Human HT-1080 fibrosarcoma cells were grafted onto the chorioallantoic membrane of fertilized chick eggs to assess the antitumoral and the antiangiogenic/antivasculogenic activity of compounds 12, 26, 31, 35, 36, 38, 44, 45, 46, and 60 in the CAM assay (Figure 2). The results shown in Figure 2 were obtained from two independent experiments using at least 10 eggs per experiment. No related toxicity was observed on chick embryos treated with the excipient. Untreated eggs were used as negative controls and for normalization of the results. The drugs

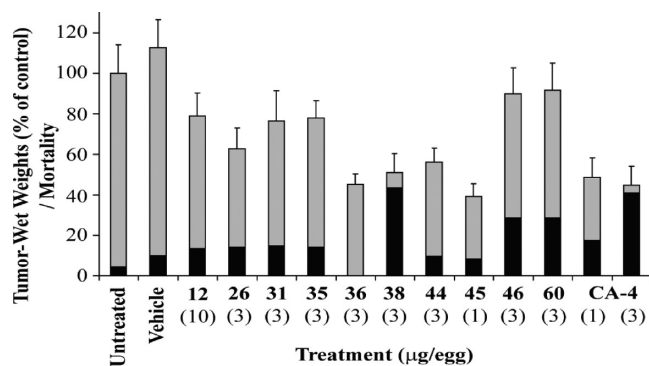


Figure 2. Effect of compounds 12, 26, 31, 35, 36, 38, 44–46, 60, and CA-4 on HT 1080 tumor growth and embryo's toxicity using the CAM model. Gray bars represent the percentage of tumor-wet weight of tumors treated with and without excipient. Black bars represent the percentage of chick embryo mortality.

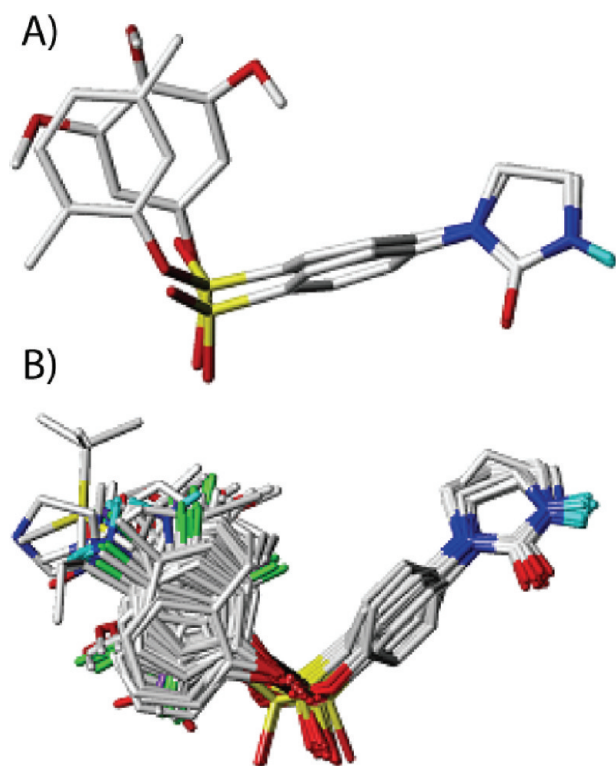


Figure 3. (A) Alignment hypothesis generated using Surfex-Sim mutual alignment module from compounds 26 and 45. (B) Superposition of the derivatives of PIB-SOs and PPB-SOs onto the alignment hypothesis.

were administered iv at 3 μg per egg except for compounds 12 and 45, which were injected at 10 and 1 μg per egg, respectively. Finally, CA-4 was used as positive control and was administered iv at 1 and 3 μg per egg.

Comparative Molecular Field and Comparative Molecular Similarity Indices Analyses (CoMFA and CoMSIA) of PIB-SOs and PPB-SOs. CoMFA and CoMSIA analyses were conducted to establish quantitative structure–activity relationships ruling the antiproliferative activity of PIB-SOs, to understand the mechanisms underlying the binding of PIB-SOs to the C-BS, and to

design new and more selective C-BS antagonists. From computational experiments, we developed 3D quantitative structure–activity relationships (3D-QSAR) models. To that end, we used Surfex-Sim which is a 3D molecular similarity optimization and searching program that uses a morphological similarity function and fast pose generation based similarity on a molecule's shape, hydrogen bonding, and electrostatic properties techniques to generate alignments of molecules.⁵² Surfex-Sim algorithm was expected to reduce the impact of factors of uncertainty during the generation of the QSAR models. The multiple alignments of most of the active compounds gave the best description of the positions of functional groups leading to the hypothesis generation. Underlying assumption in the alignment is that the compound with better fit to the hypothesis on structural alignment would have better activity. At first, a mutual alignment of the most potent compounds was performed to find a superposition of all input molecules that maximizes the similarity and minimizes the overall volume of the superposition. A hypothesis was generated from this superposition, and that hypothesis will be used as a template to align the set of active molecules. Then the alignment of the data set will be used to generate QSAR models. Compounds 26 and 45 were chosen to generate hypothesis using SYBYL Surfex-Sim mutual alignment module. The alignment hypothesis shows that the groups of same property are well aligned (Figure 3A). Then all PIB-SOs and PPB-SOs were superposed on to the alignment hypothesis using Surfex-Sim flexible superposition module (Figure 3B).

From the q^2 and r^2_{cv} values, the analysis that includes the similarity data to the hypothesis improved the r^2_{cv} in both CoMFA and CoMSIA models (models A, B, C vs models D, E, F, models G, H, I vs models J, K, L). All three antiproliferative activities in HT-29, M21, and MCF7 cell lines were then used as dependent variables to build CoMSIA and CoMFA models. The optimized parameters and the statistical data in the PLS analysis of six CoMSIA models and six CoMFA models are listed in Tables 5 and 6.

DISCUSSION

PIB-SOs Exhibit Potent Antiproliferative Activity on Tumor Cells. PIB-SO and PPB-SO derivatives were divided into four subgroups based on IC_{50} : (1) strong IC_{50} ranging from 4 to 10 nM (44 and 45); (2) good IC_{50} ranging from 8.2 to 60 nM (9, 24–26, 28, 30, 31, 33–38, 41, 42, 46, 48, and 55); (3) fair IC_{50} ranging from 24 to 220 nM (10–12, 16–22, 27, 29, 39, 43, 47, 49, 50, 52, 53, 56, 59–61, and 65); (4) weak IC_{50} ranging from 128 to >1000 nM (14, 15, 23, 32, 40, 51, 54, 57, 58, 62–64, and 66–81). Compounds 44 and 45 are almost equipotent to combretastatin A-4, which is almost 1000-fold higher than previous CEU derivatives. Table 3 shows that compounds 12, 26, 31, 35, 36, 38, 44–46, and 60 are also very potent against CHO, K562, L1210, P388D1, B16F0, DU 145, HT-1080, MDA-MB-231, SKOV3, and CEM cells.

Antiproliferative Activity of PIB-SOs on Chemoresistant Tumor Cells. Table 4 shows the antiproliferative activities of PIB-SOs 12, 26, 31, 35, 36, 38, 44–46, and 60 on drug-resistant cell lines CHO-TAX 5-6, CHO-VV 3-2, and CEM-VLB. On one hand, CHO-TAX 5-6 cells are resistant to microtubule stabilizers (e.g., paclitaxel) and hypersensitive to microtubule disruptors (e.g., colchicine, vinblastine), while CHO-VV 3-2 cell line are resistant to microtubule disruptors and hypersensitive to microtubule stabilizers.⁴⁸ On the other hand, CEM-VLB cells overexpress

Table 5. Statistical Data of QSAR Method with CoMSIA against Antiproliferative Activity on HT-29, M21, and MCF7 Cells

	CoMSIA 1			CoMSIA 2		
	model A ^a (HT-29)	model B ^a (M21)	model C ^a (MCF7)	model D ^a (HT-29)	model E ^a (M21)	model F ^a (MCF7)
fields and parameters ^b	CoMSIA FF, similarity, IM2, LogP, MW	CoMSIA FF, similarity, IM2, LogP, MW	CoMSIA FF, similarity, IM2, LogP, MW	CoMSIA FF, MR	CoMSIA FF, MR	CoMSIA FF, MR
q^2 ^c	0.684	0.660	0.670	0.618	0.619	0.569
r^2_{cv} ^d	0.697	0.668	0.680	0.612	0.609	0.551
STEP ₁₀₀ ^e	0.520	0.541	0.518	0.584	0.579	0.601
ONC ^f	6	6	6	6	6	6
SEE _{NoValidation} ^g	0.350	0.352	0.352	0.308	0.302	0.318
r^2	0.863	0.859	0.852	0.893	0.896	0.879
F^h	71.406	95.801	70.591	94.985	97.938	82.390
	(n1 = 6, n2 = 68)	(n1 = 6, n2 = 68)	(n1 = 6, n2 = 68)	(n1 = 6, n2 = 68)	(n1 = 6, n2 = 68)	(n1 = 6, n2 = 68)

^a Models A, B, and C are optimized CoMSIA models with similarity descriptor. Models D, E, and F are CoMSIA models without similarity descriptor.

^b CoMSIA FF: steric, electrostatic, hydrophobic, donor, acceptor. ^c q^2 = cross-validated correlation coefficient from LOO. ^d r^2_{cv} = cross-validated correlation coefficient (10 groups). ^e STEP = standard error of prediction. ^f ONC = optimal number of components. ^g SEE = standard error of estimate.

^h $F = r^2/(1 - r^2)$.

Table 6. Statistical Data of QSAR Method with CoMFA against Antiproliferative Activity on HT-29, M21, and MCF7 Cells

	CoMFA 1			CoMFA 2		
	model G ^a (HT-29)	model H ^a (M21)	model I ^a (MCF7)	model J ^a (HT-29)	model K ^a (M21)	model L ^a (MCF7)
fields and parameters ^b	CoMFA FF, similarity, MW	CoMFA FF, similarity, MW	CoMFA FF, similarity, MW	CoMFA FF, LogP	CoMFA FF, LogP	CoMFA FF, LogP
q^2 ^c	0.667	0.632	0.643	0.538	0.539	0.513
r^2_{cv} ^d	0.662	0.617	0.638	0.503	0.512	0.473
STEP ₁₀₀ ^e	0.537	0.561	0.539	0.637	0.632	0.634
STEP _{cv} ^e	0.541	0.573	0.543	0.661	0.651	0.660
ONC ^f	4	4	4	5	5	5
SEE _{NoValidation} ^g	0.368	0.370	0.378	0.326	0.321	0.340
r^2	0.844	0.840	0.824	0.879	0.882	0.860
F^h	94.467	91.731	82.105	100.253	102.718	84.958
	(n1 = 4, n2 = 70)	(n1 = 4, n2 = 70)	(n1 = 4, n2 = 70)	(n1 = 5, n2 = 69)	(n1 = 5, n2 = 69)	(n1 = 5, n2 = 69)

^a Models G, H, and I are optimized CoMFA models with similarity descriptor. Models J, K, and L are CoMFA models without similarity descriptor.

^b CoMFA FF: steric, electrostatic. ^c q^2 = cross-validated correlation coefficient from LOO. ^d r^2_{cv} = cross-validated correlation coefficient (10 groups).

^e STEP = standard error of prediction. ^f ONC = optimal number of components. ^g SEE = standard error of estimate. ^h $F = r^2/(1 - r^2)$.

P-glycoprotein⁵³ which is responsible for the cellular efflux of drugs and chemoresistance to anticancer drugs such as doxorubicin, etoposide, paclitaxel, and vinblastine.⁵⁴ As expected and shown in Table 4, CHO-TAX 5-6 cells that are resistant to paclitaxel were sensitive to PIB-SOs, colchicine, and vinblastine. Beside compound 44, CHO-VV 3-2 cells that are resistant to the colchicine and vinblastine were sensitive to paclitaxel and were unexpectedly sensitive to PIB-SOs. Finally, CEM-VLB cells that are 46-, 12370-, and 1579-fold resistant to the colchicine, vinblastine, and paclitaxel, respectively, were still sensitive to PIB-SOs. These results demonstrate the insensitivity of the antiproliferative activity of PIB-SOs to tubulin mutations and P-glycoprotein overexpression.

PIB-SOs Arrest Cell Cycle Progression in G₂/M Phase. Table 2 shows the percentage of M21 cells exhibiting arrest of the cell cycle progression in G₀/G₁, S, and G₂/M phases, respectively, after treatment with PIB-SOs for 24 h at 5 times their respective IC₅₀. Control cells treated with 0.5% of DMSO were found to be in G₀/G₁, S, and G₂/M phases at 61%, 30%, and 9%, respectively. Incubation with compounds 9, 11, 12, 19–22,

24, 26, 27, 30, 31, 33, 35–38, 41, 43, 44, 46–49, 53, 55, 56, and 65 strongly blocked the cell cycle in G₂/M phase; the number of cells in G₂/M phase increased by 39–86%. Compounds 10, 16, 17, 25, 28, 34, 42, 45, and 59 blocked almost exclusively the cell cycle in G₂/M phase, which is similar to the effect of CA-4.

PIB-SOs Inhibit EBI Binding to the Colchicine-Binding Site. C-BS antagonists such as colchicine, podophyllotoxin,⁵⁵ 2-methoxyestradiol,^{56,57} and CA-4 inhibit the EBI binding to β -tubulin leading to the disappearance of the β -tubulin–EBI adduct formed and detectable by Western blot as a second immunoreacting band of β -tubulin migrating faster than the native β -tubulin.⁴⁶ Control cells treated with 0.5% DMSO followed by EBI show an intense β -tubulin–EBI adduct band. With the exception of compound 11, all PIB-SO inhibited the EBI binding to the C-BS. As depicted in Table 2, compounds 12, 17, 25, 33, 47, 49, 53, 55, and 56 weakly interacted with the C-BS. However, compounds 9, 21, 27, 30, 37, and 60 strongly inhibit the formation of the β -tubulin–EBI adduct and compounds 10, 16, 19, 20, 22, 24, 26, 28, 31, 34–36, 38, 39, 41–46, 48, 59, and

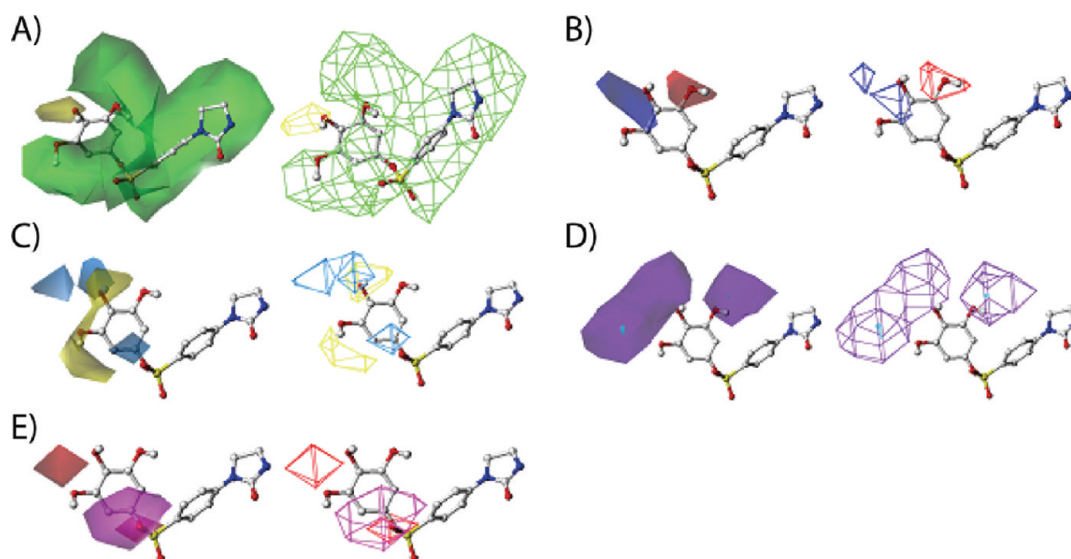


Figure 4. Contour maps of CoMSIA fields contributing to ligand binding generated by PLS analysis in model A (HT-29). Compound **45** (ball-and-stick model) was shown in the figure as a reference to depict the field region. (A) Contour map of steric field. Green areas present favored steric groups, and yellow areas present disfavored steric groups. (B) Contour map of electrostatic field. Blue areas favored electrostatic field (higher positive charge will increase the activity) and red areas disfavored electrostatic field (lower positive charge will increase the activity). (C) Contour map of hydrophobic field. Yellow areas show favored hydrophobic region, and cyan areas show disfavored hydrophobic region. (D) Contour map of hydrogen bond donor field. Cyan regions are the hydrogen bond donor preferred region, and purple regions are where hydrogen bond donor is not favored. (E) Contour map of hydrogen bond acceptor field. Magenta regions depict the favored hydrogen bond acceptor region, and red regions illustrate the hydrogen bond disfavored region.

65 abrogate its formation as CA-4 does, suggesting that these molecules are strongly binding to the C-BS and that they act as antimetotics.

PIB-SOs Disrupt the Cytoskeleton of Tumor Cells. Table 2 shows the cytoskeleton of M21 cells treated with PIB-SO at 5 times their respective IC_{50} . The cytoskeleton of control M21 cells treated with DMSO is homogeneous and linear and forms a structured network, while all the cytoskeleton of M21 cells treated with the 41 PIB-SOs tested so far clearly exhibit disrupted microtubular structures.

PIB-SOs Inhibit the Growth of Solid Tumors in the CAM Assay. The growth of solid tumors on the surface of the chorioallantoic membrane depends on the ability of the grafted tumor cells to stimulate angiogenesis and to grow significantly within a 7-day period. HT-1080 human fibrosarcoma cells were used because they produce solid tumors that are sensitive to antiangiogenic and antitumoral drugs.^{25,58–61} As shown in Figure 2, the excipient was well tolerated by chick embryos when compared to control embryos (10% and 4% mortality, respectively). The selected drugs were tested at 3 μg of drug per egg with the exception of compounds **12** and **45** which were tested also at 10 and 1 μg per egg, respectively. CA-4 was tested at 1 and 3 μg per egg and was used as a positive control exhibiting a strong anti-vasculogenic activity inhibiting tumor growth by 48% and 45%, respectively. CA-4 exhibited toxicity on chick embryos (18% and 41% mortality, respectively). Compounds **46** and **60** had no significant inhibitory effect on the growth of tumors, and both showed lethal toxicity on 29% of the embryos. Compounds **12**, **26**, **31**, and **35** weakly inhibited the growth of tumor and showed low toxicity (13–15% mortality of embryos). Compounds **36**, **44**, and **45** had good inhibition of the tumor growth higher than or similar to that of CA-4 (46%, 56%, and 39% reduction compared to controls) with almost no toxicity (0%, 10%, and

8% mortality, respectively). Finally, compound **38** strongly inhibited the growth of tumor but was toxic on 43% of the embryos.

CoMSIA Models. In all CoMSIA models, the contour map of each field has similar coverage areas for different biological activities. For example, in the contour map including HT-29, the optimized CoMSIA models included descriptors of molecular similarity (to the alignment hypothesis), molecular weight, CLogP, and the index of imidazolidin-2-one and the tetrahydropyrimidin-2(1H)-one rings (PIB-SOs and PPB-SOs). The model indicates that PIB-SOs are more preferred to contribute toward higher activity. Models without molecular similarity descriptor (models D, E, and F) had lower r^2 in both LOO analysis and cross-validation analysis. This indicates that the alignment hypothesis is reliable and the molecular similarity descriptor is required for a successful model generation. The predicted PIB-SO molecular activities of models A, B, and C are listed in Table 2 in Supporting Information.

In the set of PIB-SO molecules, the most varied position is on the phenyl ring B, so the following discussion would focus on the substitute position on this phenyl ring. Figure 4A shows the favored and disfavored areas of steric field. Most of the area surrounding the molecule was in favor of steric field. Thus, bulky groups have positive contributions to the biological activity on the phenyl group at positions 2, 3, 5, and 6. Bulky groups at position 4 have negative contribution to the biological activity. That explains why most of the compounds **52–63** have bulky substitutes on 4 positions and have lower biological activities. The effects of electrostatic field are shown in Figure 4B. As depicted in the figure, in the area around position 3 of the aromatic ring B electronegative groups increase biological activity while the electropositive group contributes to higher biological activity at positions 4 and 5. The hydrophobicity contributions are shown in Figure 4C. The most favorable areas

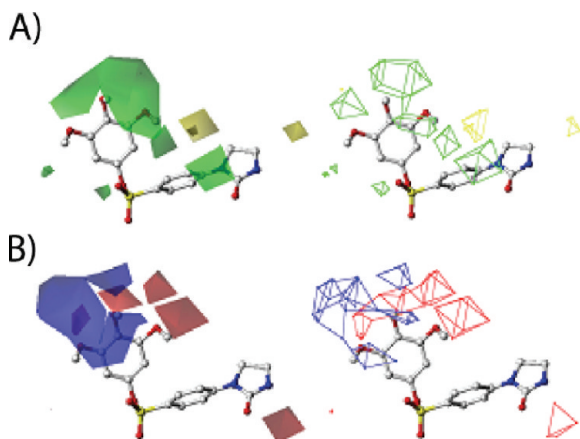


Figure 5. Contour maps of CoMFA fields contributing to ligand binding generated by PLS analysis in model G (HT-29). Compound 45 (ball-and-stick model) is shown as a reference to depict the field region. (A) Contour map of steric field. Green areas present the favored steric interaction from the ligands, and the yellow areas show the regions that disfavored steric contribution. (B) Contour map of electrostatic field. Blue areas depict favored electrostatic regions; increasing positive charge will contribute to higher activity. Red areas show the disfavored electrostatic areas, where higher ligand binding does not like higher positive charge.

for hydrophobic moieties are around position 4 and the areas of 5 and 6 positions. In the back and far end of 4 substitute positions, hydrophobic groups are not suggested. In Figure 4D, there is a very small area on the 5 substituted position that is a hydrogen bond donor preferring area (cyan color). Hydrogen bond donor was not preferred in most of the regions around 3-, 4-, and 5-substituted position (purple color). Hydrogen bond acceptor is favored in the area of sulfonate oxygen on one side of the phenyl ring (magenta color in Figure 4E). On the other side of the end group phenyl ring, around the 1 position and between 4 and 5 substituted positions are the regions for which hydrogen bond acceptor is not suggested for high biological activity (red color in Figure 4E).

CoMFA Models. In CoMFA models, we have included HT-29 activity as an example to illustrate the results shown in Figure 5. Optimized QSAR models included CoMFA fields, molecular similarity data to the hypothesis, and molecular weight. Same as CoMSIA models, molecular similarity descriptor (to the hypothesis) contributes to the successful QSAR models. The predicted PIB-SO molecular activities of models G, H, and I are listed in Table 3 in Supporting Information.

Similar to the results obtained from CoMSIA models, CoMFA models also suggested that most areas in front (the viewer side) of the phenyl ring B prefer a bulky group to make inhibitors have high biological activity (Figure 5A). But CoMFA models did not suggest the disfavored area around the 4-substituted position on the phenyl ring. There are additional areas that CoMFA models suggest to avoid the introduction of bulky groups, about 2 Å away from positions 2 and 3 of the imidazolidone ring. In Figure 5B, the favored electropositive region is much bigger than in the CoMSIA model, which covers the top and front (viewer's side) regions of 4- and 5-substituted positions of the phenyl ring. In the back of the phenyl ring (away from viewer's side), substituted 3, 4, and 5 positions of the phenyl ring preferred to have electro-negative groups. This area is also larger than the area suggested in CoMSIA models.

CONCLUSIONS

We have identified a novel class of antimicrotubule agents designated as substituted phenyl 4-(2-oxoimidazolidin-1-yl)benzenesulfonates (PIB-SOs) that bind to the C-BS on tubulin. PIB-SOs were designed as hybrid entities between CEU and CA-4 analogues where the *N*-phenyl-*N'*-(2-chloroethyl)urea pharmacophore was cyclized into a new 1-phenylimidazolidin-2-one pharmacophoric scaffold. PIB-SOs were synthesized in fair to good yields. They exhibit antiproliferative activities in the lower nanomolar range on 16 cancer cell lines and arrest the cell cycle progression in the G₂/M phase. Minor structural modifications such as expanding the five-member imidazolidin-2-one ring into the six-member tetrahydropyrimidin-2(1*H*)-one ring led to a dramatic decrease of the antiproliferative activity, indicating the sensitivity of the new pharmacophore to modifications. Competition assays using EBI and immunofluorescence using anti-β-tubulin antibody confirmed that PIB-SOs are potent antimicrotubule binding to the C-BS. In addition, the cytotoxicity of PIB-SOs was not affected in cells resistant to colchicine, paclitaxel, and vinblastine and overexpressing the P-glycoprotein. Finally, PIB-SOs 36, 44, and 45 have exhibited potent antitumoral and antiangiogenic activities in the CAM assay that are at least as good as CA-4 but exhibited also a lower toxicity than CA-4 on chick embryos, suggesting these molecules as promising anticancer drugs.

EXPERIMENTAL SECTION

Biological Methods. Cell Lines Culture. HT-29 human colon carcinoma, MCF7 human breast carcinoma, MDA-MB-231 human breast carcinoma, HT-1080 human fibrosarcoma, K562 human chronic myelogenous leukemia, L1210 murine lymphocytic leukemia, P388D1 murine macrophages, B16F0 murine melanoma, DU 145 human prostate carcinoma, and SKOV3 human ovarian were purchased from the American Type Culture Collection (Manassas, VA). Chinese hamster ovary cells (CHO), colchicine- and vinblastine-resistant CHO-VV 3-2 cells, and paclitaxel-resistant CHO-TAX 5-6 cells were generously provided by Dr. Fernando Cabral (University of Texas Medical School, Houston, TX).^{47,48} T cell leukemia CEM cells and multidrug-resistant leukemia CEM-VLB were generously provided by Dr. William T. Beck (University of Illinois at Chicago, College of Pharmacy, IL).⁴⁹ M21 human skin melanoma cells were provided by Dr. David Chershi (University of California, San Diego School of Medicine, CA). B16F0, DU 145, HT-29, HT-1080, M21, MCF7, MDA-MB-231, and SKOV3 cells were cultured in DMEM medium containing sodium bicarbonate, high glucose concentration, glutamine, and sodium pyruvate (Hyclone, Logan, UT) supplemented with 5% of calf serum. CHO, CHO-VV 3-2, CHO-TAX 5-6, CEM, CEM-VLB, K562, L1210, and P388D1 cells were cultured in RPMI medium (Hyclone, Logan, UT) supplemented with 10% of calf serum. The cells were maintained at 37 °C in a moisture-saturated atmosphere containing 5% CO₂.

Antiproliferative Activity Assay. The antiproliferative activity of PIB-SOs (9–68) and PPB-SOs (69–81) was assessed using the procedure described by the National Cancer Institute for its drug screening program with slight modifications.⁴⁵ The 96-well microtiter plates were seeded with 75 μL of tumor cell (for HT-29, 5000 cells; M21, 3500 cells; MCF7, 7500 cells; CHO, 1000 cells; K562, 5000 cells; L1210, 6000 cells; P388D1, 18 000 cells; B16F0, 2000 cells; DU 145, 5000 cells; HT-1080, 3000 cells; MDA-MB-231, 3000 cells; SKOV3, 5000 cells; CEM, 20000 cells; CHO-VV 3-2, 1000 cells; CHO-TAX 5-6, 1000 cells; CEM-VLB, 20000 cells) in appropriate medium. Plates were incubated at 37 °C, 5% CO₂ for 24 h. Freshly solubilized drugs in DMSO were diluted in fresh medium, and 75 μL aliquots containing increasing concentrations (0.98–1000 nM) of the drug were added. Plates were incubated for 48 h.

Plates containing attached cell lines were then stained with sulforhodamine B. Briefly, cells were fixed by addition of cold trichloroacetic acid to the wells (10% (w/v) final concentration), for 30 min at 4 °C. Plates were washed five times with tap water and dried. Sulforhodamine B solution (50 μ L) at 0.1% (w/v) in 1% acetic acid was added to each well, and plates were incubated for 15 min at room temperature. Unbound dye was removed by washing five times with 1% acetic acid. Bonded dye was solubilized in 10 mM Tris base, and the absorbance was read using a μ Quant Universal microplate spectrophotometer (Biotek, Winooski, VT) at a wavelength between 530 and 565 nm according to color intensity. For cells in suspension resazurin staining was used. Briefly, supernatant was aspirated and an amount of 100 μ L of resazurin at 25 μ g/mL in fresh medium was added. Plates were incubated at 37 °C for 1–3 h according to cell line sensitivity. Fluorescence was read on a FL-500 fluorometer (Biotek, Winooski, VT) using 530 nm for excitation wavelength and 590 nm for emission wavelength. The experiments were performed at least twice in triplicate. The IC₅₀ assay was considered valid when the relative standard deviation was less than 10%.

Cell Cycle Analysis. After incubation of 2.5×10^5 M21 cells with the drugs at 2 and 5 times their respective IC₅₀, for 24 h, the cells were trypsinized, washed with phosphate buffered saline (PBS), resuspended in 250 μ L of PBS, fixed by the addition of 750 μ L of ice-cold ethanol, and stored at –20 °C until use. Afterward, the cells were centrifuged for 5 min at 1000g. Cell pellets were washed with PBS and were resuspended in 450 μ L of PBS containing 200 μ g/mL RNase. After 5 min, 25 μ L of PBS containing 1 mg/mL propidium iodide was added. Mixtures were incubated on ice for 1 h, and then cell cycle distribution was analyzed using an Epics Elite ESP flow cytometer (Coulter Corporation, Miami, FL).

Inhibition of EBI-Binding to β -Tubulin. Six-well plates were seeded with MDA-MB-231 cells at 7×10^5 cells per well and incubated for 24 h. Cells were first incubated in the presence of approximately 1000 times the IC₅₀ of the drugs for 2 h, and afterward they were treated by the addition of EBI (Toronto Research Chemicals, North York, Ontario, Canada) (100 μ M, final concentration) for 1.5 h at 37 °C without changing the culture medium, which contains the drug tested. The control cells were treated with 0.5% dimethylsulfoxide. Afterward, floating and adherent cells were harvested using a rubber policeman and centrifuged for 3 min at 8000 rpm. The pellets were washed with 500 μ L of cold PBS and stored at –80 °C until use. The cells pellets were resuspended in PBS and lysed by sonication. The protein concentration was determined using the Bio-Rad protein assay (Bio-Rad Laboratories, Mississauga, Canada). Samples were diluted at 2 mg/mL protein in Laemmli buffer⁶² (60 mM Tris-Cl, pH 6.8, 2% SDS, 10% glycerol, 5% β -mercaptoethanol, 0.01% bromophenol blue). Cell extracts were boiled for 5 min. An amount of 20 μ g of proteins from the protein extracts was subjected to electrophoresis using 10% polyacrylamide gel. The proteins were transferred onto nitrocellulose membranes that were incubated with TBSMT (Tris-buffered saline + 0.1% (v/v) Tween-20 with 2.5% fat-free dry milk) for 1 h at room temperature and then with the anti- β -tubulin (clone TUB 2.1) (Sigma-Aldrich, St. Louis, MO) primary antibody in TBSMT (1:500) for 16 h at 4 °C. Membranes were washed with TBST (tris-buffered saline + 0.1% (v/v) Tween-20) and incubated with peroxidase-conjugated antimouse immunoglobulin (Amersham Canada (Oakville, Canada)) in TBSMT (1:2500) for 2.5 h at room temperature. After the membranes were washed with TBST, detection of the immunoblot was carried out with an enhanced chemiluminescence detection reagent kit provided by Amersham Canada (Oakville, Canada).

Fluorescence Microscopy. M21 cells were seeded at 1×10^5 cells per well in six-well plates that contained 22 μ m glass coverslips coated with fibronectin (10 μ g/mL) and incubated for 24 h at 37 °C. Tumor cells were incubated either with most potent PIB-SOs, CA-4, and compound 6 at 5 times their respective IC₅₀ or with DMSO (0.5%) for 16 h. Afterward, the cells were washed twice with PBS and then fixed

with 3.7% formaldehyde in PBS for 10 min. After two washes with PBS, the cells were permeabilized with 0.1% saponin in PBS and blocked with 3% (w/v) BSA in PBS for 1 h at 37 °C. The cells were then incubated for 2 h at room temperature with the anti- β -tubulin (clone TUB 2.1) in a solution containing 0.1% saponin and 3% BSA in PBS (1:200). The cells were washed five times with PBS containing 0.05% Tween-20 and incubated for 1 h at 37 °C in blocking buffer containing anti-mouse IgG Alexa-488 (Molecular Probes, Eugene, OR) (1:1000) and 4',6'-diamidino-2-phenylindole (2.5 μ g/mL in PBS) to stain the cellular nuclei (1:2000). Cells were then mounted on a microscope slide overnight with slow fade reagent (DakoCytomation, Carpinteria, CA) before analysis under a Olympus BX51 microscope. Images were captured as 8-bit tagged image format files with a Q imaging RETIGA EXI digital camera driven by Image Pro Express software.

CAM Tumor Assay. Human HT-1080 fibrosarcoma cells were used to assess the antitumoral activity of PIB-SOs in the CAM assay.^{58,59,63} Briefly, fertilized chicken eggs purchased from Couvoirs Victoriaville (Victoriaville, Québec, Canada) were incubated for 10 days in a Pro-FI egg incubator fitted with an automatic egg turner before being transferred to a Roll-X static incubator for the rest of the incubation time (incubators were purchased from Lyon Electric, Chula Vista, San Diego, CA). The eggs were kept at 37 °C in a 60% humidity atmosphere for the entire incubation period. On day 10, by use of a hobby drill (Dremel, Racine, WI), a hole was drilled on the side of the egg and a negative pressure was applied to create a new air sac. A window was opened on this new air sac and was covered with transparent adhesive tape to prevent contamination. A freshly prepared cell suspension (40 μ L) of HT-1080 (3.5×10^5 cells/egg) cells was applied directly onto the freshly exposed CAM tissue through the window. On day 11, the drugs dissolved in DMSO were extemporaneously diluted in the excipient (cremophor/ethanol 99%/PBS, 6.25/6.25/87.5 v/v). The concentration of DMSO in the excipient was kept below 0.5% to avoid its potential toxicity. The drug dissolved in 100 μ L of excipient was injected iv into 10–12 eggs. The eggs were incubated until day 17, at which time the embryos were euthanized at 4 °C followed by decapitation. Tumors were collected, and the tumor-wet weights were recorded. The number of dead embryos and signs of toxicity from the different groups were recorded.

Chemical Procedures. General. Proton NMR spectra were recorded on a Bruker AM-300 spectrometer (Bruker, Germany). Chemical shifts (δ) are reported in parts per million. IR spectra were recorded on a Magna FT-IR spectrometer (Nicolet Instrument Corporation, Madison, WI, U.S.). Uncorrected melting points were determined on an Electro-thermal melting point apparatus. HPLC analyses were performed on an Acquity UPLC sample and binary solvent manager equipped with a Quattro Premier XE tandem quadrupole mass spectrometer (Waters, Milford, MA, U.S.). A Waters BECH C18 reversed-phase column (1.7 μ m, 2.1 mm \times 50 mm, 50 °C) was eluted in 7 min with a methanol/water linear gradient containing 0.1% TFA at 0.6 mL/min. The purity of the final compounds was greater than 95%. All reactions were conducted under a dried nitrogen atmosphere. Chemicals were supplied by Aldrich Chemicals (Milwaukee, WI, U.S.) or VWR International (Mont-Royal, Québec, Canada). Liquid flash chromatography was performed on silica gel F60, 60 A, 40–63 μ m supplied by Silicycle (Québec, Canada) using a FPX flash purification system (Biotage, Charlottesville, VA, U.S.) and using the indicated solvent mixture expressed as volume/volume ratios. Solvents and reagents were used without purification unless specified otherwise. The progress of all reactions was monitored using TLC on precoated silica gel plates 60 F254 (VWR International, Mont-Royal, Québec, Canada). The chromatograms were viewed under UV light at 254 and/or 265 nm.

General Preparation of Compounds 9–81. Method A. To a stirred solution of the appropriate *N*-phenyl-*N'*-(2-chloroethyl)urea derivative (0.4 mmol) in acetonitrile (10 mL) a mixture of aluminum

oxide and potassium fluoride (6:4) (4.0 mmol) was added. The suspension was refluxed overnight. After cooling, the mixture was filtered and the solvent evaporated under reduced pressure. The residue was purified by recrystallization or flash chromatography on silica gel.

Method B. 4-(2-Oxoimidazolidin-1-yl)benzene-1-sulfonyl chloride or 4-(tetrahydro-2-oxopyrimidin-1(2H)-yl)benzene-1-sulfonyl chloride (8.00 mmol) was suspended in dry methylene chloride (10 mL) under nitrogen atmosphere. Appropriate phenol (8.00 mmol) and triethylamine (8.00 mmol) were successively added dropwise, and the mixture was stirred at room temperature for 24 h. The mixture was evaporated and the residue dissolved with ethyl acetate (100 mL). The solution was washed with hydrochloric acid 1 N (100 mL), sodium hydroxide 1 N (100 mL), brine (100 mL), dried over sodium sulfate, filtered, and evaporated to dryness under vacuum. The residue was purified by flash chromatography on silica gel.

Method C. A mixture of the appropriate nitro compound **39**, **50**, or **62** (1 equiv) dissolved in ethanol 99% (30 mL) was added dropwise Pd/C 10% (0.02 equiv). The nitro compound was reduced under hydrogen atmosphere (38 psi) overnight. The catalyst was removed by filtration, and the filtrate was evaporated to dryness. The residue was purified by flash chromatography on silica gel to give compounds **40**, **51**, and **63**.

2-Tolyl-4-(2-oxoimidazolidin-1-yl)benzenesulfonate (9). Method A: recrystallization from methylene chloride/hexanes 1:20. Yield: 88%. Method B: flash chromatography (methylene chloride to methylene chloride/ethyl acetate 8:2). Yield: 95%. White solid. Mp: 166–167 °C. IR ν : 3242, 1715 cm^{-1} . ^1H NMR (DMSO- d_6): δ 7.84–7.69 (m, 4H, Ar), 7.44 (s, 1H, NH), 7.31–7.20 (m, 3H, Ar), 7.00–6.96 (m, 1H, Ar), 3.96–3.91 (m, 2H, CH_2), 3.49–3.44 (m, 2H, CH_2), 2.04 (s, 3H, CH_3). ^{13}C NMR (DMSO- d_6): δ 158.2, 147.9, 146.2, 131.7, 131.0, 129.3, 127.3, 127.2, 126.0, 122.0, 116.4, 44.3, 36.3, 15.9. HRMS (ES+) m/z found 333.0889; $\text{C}_{16}\text{H}_{16}\text{N}_2\text{O}_4\text{S}$ (M^+ + H) requires 333.0909.

3-Tolyl-4-(2-oxoimidazolidin-1-yl)benzenesulfonate (10). Method A: flash chromatography (methylene chloride to methylene chloride/ethyl acetate 8:2). Yield: 56%. Method B: flash chromatography (methylene chloride to methylene chloride/ethyl acetate 8:10). Yield: 97%. White solid. Mp: 168–169 °C. IR ν : 3217, 1704 cm^{-1} . ^1H NMR (CDCl_3): δ 7.78–7.68 (m, 4H, Ar), 7.16–7.10 (m, 1H, Ar), 7.04–7.02 (m, 1H, Ar), 6.88 (s, 1H, Ar), 6.73–6.70 (m, 1H, Ar), 5.40 (brs, 1H, NH), 4.00–3.95 (m, 2H, CH_2), 3.67–3.61 (m, 2H, CH_2), 2.29 (s, 3H, CH_3). ^{13}C NMR (CDCl_3): δ 159.2, 149.6, 145.3, 140.0, 129.6, 129.2, 127.9, 127.6, 122.9, 119.1, 116.6, 44.8, 37.1, 21.2. HRMS (ES+) m/z found 333.0354; $\text{C}_{16}\text{H}_{16}\text{N}_2\text{O}_4\text{S}$ (M^+ + H) requires 333.0909.

4-Tolyl-4-(2-oxoimidazolidin-1-yl)benzenesulfonate (11). Method A: recrystallization from methylene chloride/hexanes 1:20. Yield: 81%. Method B: flash chromatography (methylene chloride to methylene chloride/ethyl acetate 8:2). Yield: 97%. White solid. Mp: 192–193 °C. IR ν : 3252, 1713 cm^{-1} . ^1H NMR (DMSO- d_6): δ 7.80–7.70 (m, 4H, Ar), 7.40 (s, 1H, NH), 7.15 (d, 2H, $J = 8.3$ Hz, Ar), 6.87 (d, 2H, $J = 8.3$ Hz, Ar), 3.93–3.87 (m, 2H, CH_2), 3.46–3.41 (m, 2H, CH_2), 2.25 (s, 3H, CH_3). ^{13}C NMR (DMSO- d_6): δ 163.4, 152.2, 151.3, 142.0, 135.5, 134.6, 130.5, 127.0, 121.5, 49.4, 41.5, 25.6. HRMS (ES+) m/z found 333.0380; $\text{C}_{16}\text{H}_{16}\text{N}_2\text{O}_4\text{S}$ (M^+ + H) requires 333.0909.

4-Methoxyphenyl-4-(2-oxoimidazolidin-1-yl)benzenesulfonate (12). Method A: flash chromatography (methylene chloride to methylene chloride/ethyl acetate 8:2). Yield: 62%. Method B: flash chromatography (methylene chloride to methylene chloride/ethyl acetate 8:2). Yield: 75%. White solid. Mp: 178–179 °C. IR ν : 3244, 1709 cm^{-1} . ^1H NMR (CDCl_3 and MeOD): δ 7.68–7.60 (m, 4H, Ar), 6.82–6.79 (m, 2H, Ar), 6.72–6.69 (m, 2H, Ar), 3.94–3.89 (m, 2H, CH_2), 3.70 (s, 3H, CH_3), 3.58–3.53 (m, 2H, CH_2). ^{13}C NMR (CDCl_3 and MeOD): δ 159.1, 158.2, 145.3, 143.0, 129.6, 127.3, 123.3, 116.6, 114.5, 55.5, 44.8, 37.0. HRMS (ES+) m/z found 349.0853; $\text{C}_{16}\text{H}_{16}\text{N}_2\text{O}_5\text{S}$ (M^+ + H) requires 349.0858.

4-(Dimethylamino)phenyl-4-(2-oxoimidazolidin-1-yl)benzenesulfonate (13). Method A: flash chromatography (methylene chloride to methylene chloride/ethyl acetate 8:2). Yield: 53%. Method B: flash chromatography (methylene chloride to methylene chloride/ethyl acetate (8:2)). Yield: 17%. White solid. Mp: 206–207 °C. IR ν : 2805, 1711 cm^{-1} . ^1H NMR (CDCl_3 and MeOD): δ 7.64–7.55 (m, 4H, Ar), 6.79 (d, 2H, $J = 9.1$ Hz, Ar), 6.52 (d, 2H, $J = 9.1$ Hz, Ar), 3.90–3.85 (m, 2H, CH_2), 3.54–3.48 (m, 3H, CH_2 and NH), 2.80 (s, 6H, 2 \times CH_3). ^{13}C NMR (CDCl_3 and MeOD): δ 158.9, 149.3, 145.0, 140.3, 129.7, 128.1, 122.9, 116.6, 112.6, 44.8, 40.6, 37.0. HRMS (ES+) m/z found 362.0071; $\text{C}_{17}\text{H}_{19}\text{N}_3\text{O}_4\text{S}$ (M^+ + H) requires 362.1175.

4-Hydroxyphenyl-4-(2-oxoimidazolidin-1-yl)benzenesulfonate (14). Method A: flash chromatography (methylene chloride/ethyl acetate/methanol 8:2:0 to 75:20:5). Yield: 35%. To a stirred solution of **58** (1 equiv) in tetrahydrofuran (10 mL) was added tetrabutylammonium fluoride 1 M in tetrahydrofuran (1.1 equiv). The mixture was stirred overnight. Then hydrochloric acid was added, the appropriate layer was extracted with 3 \times ethyl acetate, washed with brine, and dried with sodium sulfate, and the solvent was evaporated under reduced pressure to afford **14**. Yield: 99%. White solid. Mp: 241–242 °C. IR ν : 3440, 1686 cm^{-1} . ^1H NMR (DMSO- d_6): δ 9.67 (s, 1H, OH), 7.81–7.69 (m, 4H, Ar), 7.41 (s, 1H, NH), 6.80–6.67 (m, 4H, Ar), 3.94–3.89 (m, 2H, CH_2), 3.48–3.42 (m, 2H, CH_2). ^{13}C NMR (DMSO- d_6): δ 158.2, 157.0, 146.0, 140.9, 129.4, 125.4, 123.0, 116.3, 116.0, 44.2, 36.3. HRMS (ES+) m/z found 334.9951; $\text{C}_{15}\text{H}_{14}\text{N}_2\text{O}_5\text{S}$ (M^+ + H) requires 335.0702.

Phenyl-4-(2-oxoimidazolidin-1-yl)benzenesulfonate (15). Method B: flash chromatography (ethyl acetate to ethyl acetate/methanol 95:5). Yield: 75%. White solid. Mp: 149–151 °C. IR ν : 3262, 1713 cm^{-1} . ^1H NMR (DMSO- d_6): δ 7.82–7.73 (m, 4H, Ar), 7.41–7.29 (m, 4H, Ar or NH), 7.03 (s, 1H, Ar or NH), 7.01 (s, 1H, Ar or NH), 3.94–3.89 (m, 2H, CH_2), 3.48–3.43 (m, 2H, CH_2). ^{13}C NMR (DMSO- d_6): δ 158.2, 149.2, 146.1, 130.0, 129.4, 127.4, 125.3, 122.1, 116.3, 44.2, 36.3. HRMS (ES+) m/z found 319.0589; $\text{C}_{15}\text{H}_{14}\text{N}_2\text{O}_4\text{S}$ (M^+ + H) requires 319.0753.

2-Ethylphenyl-4-(2-oxoimidazolidin-1-yl)benzenesulfonate (16). Method B: flash chromatography (methylene chloride to methylene chloride/ethyl acetate 8:2). Yield: 48%. White solid. Mp: 163–164 °C. IR ν : 3264, 1712 cm^{-1} . ^1H NMR (CDCl_3 and DMSO- d_6): δ 7.42–7.35 (m, 4H, Ar), 6.88–6.83 (m, 1H, Ar), 6.75–6.73 (m, 1H, Ar), 6.52 (brs, 1H, NH), 6.46–6.41 (m, 2H, Ar), 3.64–3.59 (m, 2H, CH_2), 3.28–3.23 (m, 2H, CH_2), 2.25 (q, 2H, $J = 7.6$ Hz, CH_2), 0.82 (t, 3H, $J = 7.6$ Hz, CH_3). ^{13}C NMR (CDCl_3 and DMSO- d_6): δ 158.9, 148.0, 145.3, 137.3, 129.8, 129.5, 128.6, 127.1, 126.8, 122.1, 116.7, 44.9, 37.1, 22.8, 14.1. HRMS (ES+) m/z found 347.0495; $\text{C}_{17}\text{H}_{18}\text{N}_2\text{O}_4\text{S}$ (M^+ + H) requires 347.1066.

2-Propylphenyl-4-(2-oxoimidazolidin-1-yl)benzenesulfonate (17). Method B: flash chromatography (methylene chloride to methylene chloride/ethyl acetate 8:2). Yield: 90%. White solid. Mp: 153–154 °C. IR ν : 3235, 1714 cm^{-1} . ^1H NMR (CDCl_3 and DMSO- d_6): δ 7.38–7.35 (m, 4H, Ar), 6.83–6.72 (m, 3H, Ar), 6.63–6.61 (m, 1H, Ar), 6.56 (s, 1H, NH), 3.61–3.56 (m, 2H, CH_2), 3.24–3.19 (m, 2H, CH_2), 2.05 (t, 2H, $J = 7.7$ Hz, CH_2), 1.20–1.07 (m, 2H, CH_2), 0.50 (t, 3H, $J = 7.3$ Hz, CH_3). ^{13}C NMR (CDCl_3 and DMSO- d_6): δ 158.2, 147.6, 146.2, 135.1, 130.8, 129.2, 127.3, 127.2, 126.1, 121.8, 116.4, 44.3, 36.3, 31.2, 22.6, 13.8. HRMS (ES+) m/z found 361.0658; $\text{C}_{18}\text{H}_{20}\text{N}_2\text{O}_4\text{S}$ (M^+ + H) requires 361.1222.

2-Methoxyphenyl-4-(2-oxoimidazolidin-1-yl)benzenesulfonate (18). Method B: flash chromatography (ethyl acetate to ethyl acetate/methanol 95:5). Yield: 76%. White solid. Mp: 183–185 °C. IR ν : 3236, 1715 cm^{-1} . ^1H NMR (DMSO- d_6): δ 7.81–7.71 (m, 4H, Ar), 7.40 (s, 1H, NH), 7.29–7.24 (m, 1H, Ar), 7.08–7.05 (m, 2H, Ar), 6.96–6.91 (m, 1H, Ar), 3.95–3.90 (m, 2H, CH_2), 3.55 (s, 3H, CH_3), 3.49–3.44 (m, 2H, CH_2). ^{13}C NMR (DMSO- d_6): δ 158.3, 151.5, 146.0,

137.7, 129.4, 128.4, 126.2, 123.4, 120.6, 116.0, 113.4, 55.6, 44.3, 36.3. HRMS (ES⁺) *m/z* found 349.0858; C₁₆H₁₆N₂O₅S (M⁺ + H) requires 348.9406.

2-Ethoxyphenyl-4-(2-oxoimidazolidin-1-yl)benzenesulfonate (19). Method B: flash chromatography (ethyl acetate to ethyl acetate/methanol 95:5). Yield: 64%. White solid. Mp: 169–171 °C. IR *v*: 3236, 2907, 1713 cm⁻¹. ¹H NMR (DMSO-*d*₆): δ 7.81–7.70 (m, 4H, Ar), 7.40 (brs, 1H, NH), 7.27–7.22 (m, 1H, Ar), 7.14–7.12 (m, 1H, Ar), 7.05–7.02 (m, 1H, Ar), 6.96–6.91 (m, 1H, Ar), 3.94–3.89 (m, 2H, CH₂), 3.81 (q, 2H, *J* = 7.0 Hz, CH₂), 3.46 (m, 2H, CH₂), 1.16 (t, 3H, *J* = 7.0 Hz, CH₃). ¹³C NMR (DMSO-*d*₆): δ 158.2, 150.7, 146.0, 137.7, 129.3, 128.3, 126.3, 123.6, 120.4, 116.1, 114.1, 63.8, 44.3, 36.3, 14.3. HRMS (ES⁺) *m/z* found 362.9793; C₁₇H₁₈N₂O₅S (M⁺ + H) requires 363.1015.

2-Chlorophenyl-4-(2-oxoimidazolidin-1-yl)benzenesulfonate (20). Method B: flash chromatography (ethyl acetate to ethyl acetate/methanol 95:5). Yield: 86%. White solid. Mp: 167–169 °C. IR *v*: 3255, 2909, 1709 cm⁻¹. ¹H NMR (DMSO-*d*₆): δ 7.85–7.78 (m, 4H, Ar), 7.58–7.54 (m, 1H, Ar), 7.43–7.33 (m, 3H, Ar and NH), 7.27–7.24 (m, 1H, Ar), 3.96–3.91 (m, 2H, CH₂), 3.49–3.43 (m, 2H, CH₂). ¹³C NMR (DMSO-*d*₆): δ 158.2, 146.5, 145.0, 130.9, 129.6, 128.7, 126.5, 125.3, 123.9, 116.4, 44.3, 36.3. HRMS (ES⁺) *m/z* found 353.0363; C₁₅H₁₃ClN₂O₄S (M⁺ + H) requires 353.0159.

2-Fluorophenyl-4-(2-oxoimidazolidin-1-yl)benzenesulfonate (21). Method B: flash chromatography (ethyl acetate to ethyl acetate/methanol 95:5). Yield: 67%. White solid. Mp: 164–166 °C. IR *v*: 3217, 2905, 1698 cm⁻¹. ¹H NMR (DMSO-*d*₆): δ 7.85–7.76 (m, 4H, Ar), 7.45 (brs, 1H, NH), 7.38–7.33 (m, 2H, Ar), 7.26–7.14 (m, 2H, Ar), 3.96–3.91 (m, 2H, CH₂), 3.49–3.44 (m, 2H, CH₂). ¹³C NMR (DMSO-*d*₆): δ 158.2, 146.5, 129.5, 129.1, 129.0, 125.4, 125.3, 124.9, 124.6, 117.5, 117.2, 116.4, 44.3, 36.3. HRMS (ES⁺) *m/z* found 337.0649; C₁₅H₁₃FN₂O₄S (M⁺ + H) requires 337.0658.

2-Iodophenyl-4-(2-oxoimidazolidin-1-yl)benzenesulfonate (22). Method B: flash chromatography (ethyl acetate to ethyl acetate/methanol 95:5). Yield: 73%. White solid. Mp: 205–207 °C. IR *v*: 3226, 2913, 1703 cm⁻¹. ¹H NMR (DMSO-*d*₆ and CDCl₃): δ 7.74–7.72 (m, 5H, Ar), 7.33–7.28 (m, 1H, Ar), 7.19–7.17 (m, 1H, Ar), 7.11 (brs, 1H, NH), 6.99–6.94 (m, 1H, Ar), 3.93–3.88 (m, 2H, CH₂), 3.53–3.48 (m, 2H, CH₂). ¹³C NMR (DMSO-*d*₆ and CDCl₃): δ 158.2, 149.5, 146.1, 139.7, 129.4, 129.3, 128.2, 126.1, 122.3, 116.0, 90.3, 44.2, 36.4. HRMS (ES⁺) *m/z* found 444.9523; C₁₅H₁₃IN₂O₄S (M⁺ + H) requires 444.9719.

2-Nitrophenyl-4-(2-oxoimidazolidin-1-yl)benzenesulfonate (23). Method B: flash chromatography (methylene chloride to methylene chloride/ethyl acetate 0:1). Yield: 83%. White solid. Mp: 181–182 °C. IR *v*: 3423, 3113, 1710 cm⁻¹. ¹H NMR (CDCl₃, MeOD and DMSO-*d*₆): δ 7.22–7.16 (m, 1H, Ar), 7.06–7.03 (m, 2H, Ar), 6.97–6.88 (m, 3H, Ar), 6.79–6.73 (m, 1H, Ar), 6.45–6.43 (m, 1H, Ar), 3.24–3.19 (m, 2H, CH₂), 8.82–2.77 (m, 2H, CH₂). ¹³C NMR (CDCl₃, MeOD and DMSO-*d*₆): δ 158.5, 146.7, 143.2, 141.1, 134.5, 129.5, 128.0, 125.8, 125.0, 124.9, 116.5, 44.5, 36.6. HRMS (ES⁺) *m/z* found 363.9450; C₁₅H₁₃N₃O₆S (M⁺ + H) requires 364.0603.

2,3-Dimethylphenyl-4-(2-oxoimidazolidin-1-yl)benzenesulfonate (24). Method B: flash chromatography (ethyl acetate to ethyl acetate/methanol 95:5). Yield: 72%. White solid. Mp: 190–192 °C. IR *v*: 3242, 3118, 1716 cm⁻¹. ¹H NMR (DMSO-*d*₆ and CDCl₃): δ 7.75–7.65 (m, 4H, Ar), 7.17 (brs, 1H, NH), 7.02–6.94 (m, 2H, Ar), 6.74–6.72 (m, 1H, Ar), 3.93–3.89 (m, 2H, CH₂), 3.53–3.48 (m, 2H, CH₂), 2.19 (s, 3H, CH₃), 1.93 (s, 3H, CH₃). ¹³C NMR (DMSO-*d*₆ and CDCl₃): δ 158.3, 147.8, 145.8, 138.6, 129.7, 128.9, 128.0, 126.6, 125.7, 119.3, 116.0, 44.2, 36.5, 19.7, 12.4. HRMS (ES⁺) *m/z* found 347.1050; C₁₇H₁₈N₂O₄S (M⁺ + H) requires 347.1066.

2,4-Dimethylphenyl-4-(2-oxoimidazolidin-1-yl)benzenesulfonate (25). Method B: flash chromatography (methylene chloride

to methylene chloride/ethyl acetate 8:2). Yield: 98%. White solid. Mp: 203–204 °C. IR *v*: 3228, 1714 cm⁻¹. ¹H NMR (DMSO-*d*₆): δ 7.84–7.74 (m, 4H, Ar), 7.44 (s, 1H, NH), 7.07–6.99 (m, 2H, Ar), 6.83–6.81 (m, 1H, Ar), 3.96–3.90 (m, 2H, CH₂), 3.49–3.43 (m, 2H, CH₂), 2.25 (s, 3H, CH₃), 1.98 (s, 3H, CH₃). ¹³C NMR (DMSO-*d*₆): δ 158.2, 146.1, 145.7, 136.5, 132.1, 130.6, 129.3, 127.6, 126.0, 121.7, 116.4, 44.3, 36.3, 20.3, 15.8. HRMS (ES⁺) *m/z* found 347.0571; C₁₇H₁₈N₂O₄S (M⁺ + H) requires 347.1066.

2,5-Dimethylphenyl-4-(2-oxoimidazolidin-1-yl)benzenesulfonate (26). Method B: flash chromatography (ethyl acetate to ethyl acetate/methanol 95:5). Yield: 76%. White solid. Mp: 184–186 °C. IR *v*: 3241, 1710 cm⁻¹. ¹H NMR (DMSO-*d*₆): δ 7.84–7.76 (m, 4H, Ar), 7.41 (brs, 1H, NH), 7.15–7.13 (m, 1H, Ar), 7.05–7.02 (m, 1H, Ar), 6.86 (s, 1H, Ar), 3.95–3.90 (m, 2H, CH₂), 3.49–3.43 (m, 2H, CH₂), 2.24 (s, 3H, CH₃), 1.94 (s, 3H, CH₃). ¹³C NMR (DMSO-*d*₆): δ 158.2, 147.6, 146.2, 136.8, 131.3, 129.2, 127.8, 127.6, 126.1, 122.5, 116.4, 44.3, 36.3, 20.4, 15.4. HRMS (ES⁺) *m/z* found 347.1051; C₁₇H₁₈N₂O₄S (M⁺ + H) requires 347.1066.

2,4,5-Trimethylphenyl-4-(2-oxoimidazolidin-1-yl)benzenesulfonate (27). Method B: flash chromatography (ethyl acetate to ethyl acetate/methanol 95:5). Yield: 69%. White solid. Mp: 204–205 °C. IR *v*: 3232, 2917, 1710 cm⁻¹. ¹H NMR (DMSO-*d*₆ and CDCl₃): δ 7.74–7.64 (m, 4H, Ar), 7.16 (brs, 1H, NH), 6.86 (s, 1H, Ar), 6.71 (s, 1H, Ar), 3.93–3.88 (m, 2H, CH₂), 3.53–3.48 (m, 2H, CH₂), 2.13 (s, 3H, CH₃), 2.11 (s, 3H, CH₃), 1.88 (s, 3H, CH₃). ¹³C NMR (DMSO-*d*₆ and CDCl₃): δ 158.3, 145.7, 145.6, 134.8, 134.8, 132.1, 128.9, 127.5, 126.8, 122.7, 116.0, 44.2, 36.5, 19.0, 18.7, 15.3. HRMS (ES⁺) *m/z* found 361.1190; C₁₈H₂₀N₂O₄S (M⁺ + H) requires 361.1222.

2,4,5-Trichlorophenyl-4-(2-oxoimidazolidin-1-yl)benzenesulfonate (28). Method B: flash chromatography (methylene chloride to methylene chloride/ethyl acetate 8:2). Yield: 62%. White solid. Mp: 186–187 °C. IR *v*: 3204, 1710 cm⁻¹. ¹H NMR (DMSO-*d*₆): δ 8.03 (s, 1H, Ar), 7.84–7.83 (m, 4H, Ar), 7.60 (s, 1H, Ar), 7.47 (brs, 1H, NH), 3.96–3.91 (m, 2H, CH₂), 3.49–3.44 (m, 2H, CH₂). ¹³C NMR (DMSO-*d*₆): δ 158.1, 146.9, 144.0, 131.7, 130.9, 130.7, 129.8, 126.6, 125.7, 124.5, 116.5, 44.3, 36.3. HRMS (ES⁺) *m/z* found 420.8198; C₁₅H₁₁Cl₃N₂O₄S (M⁺ + H) requires 420.9583.

2,4,6-Trichlorophenyl-4-(2-oxoimidazolidin-1-yl)benzenesulfonate (29). Method B: flash chromatography (methylene chloride to methylene chloride/ethyl acetate 7:3). Yield: 75%. White solid. Mp: 254–255 °C. IR *v*: 3202, 1711 cm⁻¹. ¹H NMR (CDCl₃ + MeOD): δ 7.92 (d, 2H, *J* = 9.0 Hz, Ar), 7.73 (d, 2H, *J* = 9.0 Hz, Ar), 7.33 (s, 2H, Ar), 4.01–3.96 (m, 2H, CH₂), 3.64–3.59 (m, 2H, CH₂). ¹³C NMR (CDCl₃ + MeOD): δ 159.9, 149.8, 145.7, 137.7, 130.9, 129.8, 129.1, 119.6, 116.7, 44.8, 36.9. HRMS (ES⁺) *m/z* found 420.9216; C₁₅H₁₁Cl₃N₂O₄S (M⁺ + H) requires 420.9583.

2,4-Difluorophenyl-4-(2-oxoimidazolidin-1-yl)benzenesulfonate (30). Method B: flash chromatography (ethyl acetate to ethyl acetate/methanol 95:5). Yield: 85%. White solid. Mp: 179–183 °C. IR *v*: 3236, 1722 cm⁻¹. ¹H NMR (DMSO-*d*₆ and CDCl₃): δ 7.73–7.64 (m, 4H, Ar), 7.09–6.80 (m, 3H, Ar), 5.06 (br s, 1H, NH), 3.93–3.88 (m, 2H, CH₂), 3.54–3.49 (m, 2H, CH₂). ¹³C NMR (DMSO-*d*₆ and CDCl₃): δ 158.2, 146.1, 129.1, 126.3, 125.2, 125.0, 116.0, 115.8, 111.4, 111.4, 111.1, 105.5, 105.2, 105.1, 104.8, 44.2, 36.4. HRMS (ES⁺) *m/z* found 355.0443; C₁₅H₁₂F₂N₂O₄S (M⁺ + H) requires 355.0564.

2,6-Difluorophenyl-4-(2-oxoimidazolidin-1-yl)benzenesulfonate (31). Method B: flash chromatography (ethyl acetate to ethyl acetate/methanol 95:5). Yield: 81%. White solid. Mp: 187–189 °C. IR *v*: 3240, 1732 cm⁻¹. ¹H NMR (DMSO-*d*₆ and CDCl₃): δ 7.75 (s, 4H, Ar), 7.27–7.17 (m, 2H, Ar or NH), 7.00–6.95 (m, 2H, Ar or NH), 3.95–3.90 (m, 2H, CH₂), 3.54–3.49 (m, 2H, CH₂). ¹³C NMR (DMSO-*d*₆ and CDCl₃): δ 158.2, 157.2, 157.1, 153.8, 153.8, 146.2, 129.1, 127.8, 127.7, 127.6, 125.7, 125.6, 116.1, 112.4, 112.4, 112.4, 112.2, 112.2, 112.1,

44.2, 36.4. HRMS (ES⁺) *m/z* found 355.0549; C₁₅H₁₂F₂N₂O₄S (M⁺ + H) requires 355.0564.

Perfluorophenyl-4-(2-oxoimidazolidin-1-yl)benzenesulfonate (32). Method B: flash chromatography (methylene chloride to methylene chloride/ethyl acetate 8:2). Yield: 75%. White solid. Mp: 217–218 °C. IR *v*: 3258, 1711 cm⁻¹. ¹H NMR (DMSO-*d*₆): δ 7.93–7.86 (m, 4H, Ar), 7.51 (brs, 1H, NH), 3.99–3.94 (m, 2H, CH₂), 3.50–3.45 (m, 2H, CH₂). ¹³C NMR (CDCl₃ and MeOD): δ 164.2, 146.4, 146.3, 129.8, 116.9, 116.8, 44.8, 36.8. HRMS (ES⁺) *m/z* found 409.0188; C₁₅H₉F₅N₂O₄S (M⁺ + H) requires 409.0282.

3-Propylphenyl-4-(2-oxoimidazolidin-1-yl)benzenesulfonate (33). Method B: flash chromatography (ethyl acetate to ethyl acetate/methanol 95:5). Yield: 80%. White solid. Mp: 144–145 °C. IR *v*: 3257, 2951, 1714 cm⁻¹. ¹H NMR (DMSO-*d*₆ and CDCl₃): δ 7.72–7.60 (m, 4H, Ar), 7.18–7.12 (m, 2H, Ar and NH), 7.02–7.00 (m, 1H, Hz, Ar), 6.73–6.68 (m, 2H, Ar), 3.91–3.86 (m, 2H, CH₂), 3.52–3.47 (m, 2H, CH₂), 2.46 (t, 2H, J = 7.7 Hz, CH₂), 1.47 (m, 2H, CH₂), 0.79 (t, 3H, J = 7.3 Hz, CH₃). ¹³C NMR (DMSO-*d*₆ and CDCl₃): δ 158.2, 149.1, 145.7, 144.2, 129.0, 126.9, 125.9, 121.8, 119.1, 116.0, 44.2, 36.9, 36.4, 23.7, 13.2. HRMS (ES⁺) *m/z* found 361.1315; C₁₈H₂₀N₂O₄S (M⁺ + H) requires 361.1222.

3-Methoxyphenyl-4-(2-oxoimidazolidin-1-yl)benzenesulfonate (34). Method B: flash chromatography (methylene chloride to methylene chloride/ethyl acetate 8:2). Yield: 70%. White solid. Mp: 139–140 °C. IR *v*: 3219, 1712 cm⁻¹. ¹H NMR (CDCl₃ and MeOD): δ 7.73–7.62 (m, 4H, Ar), 7.13–7.08 (m, 1H, Ar), 6.74–6.71 (m, 1H, Ar), 6.54–6.47 (m, 2H, Ar), 3.93–3.89 (m, 2H, CH₂), 3.68 (s, 3H, CH₃), 3.59–3.54 (m, 2H, CH₂), 2.60 (s, 1H, NH). ¹³C NMR (CDCl₃ and MeOD): δ 160.4, 159.1, 150.5, 145.4, 129.9, 129.6, 127.5, 116.6, 114.3, 113.0, 108.3, 55.5, 44.8, 36.9. HRMS (ES⁺) *m/z* found 348.9994; C₁₆H₁₆N₂O₅S (M⁺ + H) requires 349.0858.

3-Ethoxyphenyl-4-(2-oxoimidazolidin-1-yl)benzenesulfonate (35). Method B: flash chromatography (ethyl acetate to ethyl acetate/methanol 95:5). Yield: 81%. White solid. Mp: 143–145 °C. IR *v*: 3255, 2898, 1713 cm⁻¹. ¹H NMR (DMSO-*d*₆ and CDCl₃): δ 7.79–7.63 (m, 4H, Ar), 7.16–7.09 (m, 2H, Ar and NH), 6.75–6.71 (m, 1H, Ar), 6.47–6.42 (m, 2H, Ar), 3.92–3.86 (m, 4H, 2 × CH₂), 3.53–3.47 (m, 2H, CH₂), 1.30 (t, 3H, J = 6.9 Hz, CH₃). ¹³C NMR (DMSO-*d*₆ and CDCl₃): δ 159.3, 158.2, 150.0, 145.8, 129.6, 129.0, 125.9, 116.0, 113.6, 113.0, 108.4, 63.3, 44.2, 36.5, 14.3. HRMS (ES⁺) *m/z* found 363.1002; C₁₇H₁₈N₂O₅S (M⁺ + H) requires 363.1015.

3-Chlorophenyl-4-(2-oxoimidazolidin-1-yl)benzenesulfonate (36). Method B: flash chromatography (ethyl acetate to ethyl acetate/methanol 95:5). Yield: 77%. White solid. Mp: 160–162 °C. IR *v*: 3223, 1707 cm⁻¹. ¹H NMR (DMSO-*d*₆): δ 7.85–7.77 (m, 4H, Ar), 7.46–7.42 (m, 3H, Ar), 7.20 (s, 1H, NH), 7.02–6.98 (m, 1H, Ar), 3.96–3.90 (m, 2H, CH₂), 3.49–3.44 (m, 2H, CH₂). ¹³C NMR (DMSO-*d*₆): δ 158.2, 149.6, 146.4, 133.7, 131.4, 129.5, 127.6, 124.7, 122.5, 121.0, 116.4, 44.2, 36.3. HRMS (ES⁺) *m/z* found 353.0349; C₁₅H₁₃ClN₂O₄S (M⁺ + H) requires 353.0363.

3-Fluorophenyl-4-(2-oxoimidazolidin-1-yl)benzenesulfonate (37). Method B: flash chromatography (methylene chloride to methylene chloride/ethyl acetate 8:2). Yield: 56%. White solid. Mp: 157–158 °C. IR *v*: 3243, 1712 cm⁻¹. ¹H NMR (CDCl₃ and MeOD): δ 7.68–7.58 (m, 4H, Ar), 7.21–7.13 (m, 1H, Ar), 6.91–6.85 (m, 1H, Ar), 6.71–6.66 (m, 2H, Ar), 3.91–3.86 (m, 2H, CH₂), 3.54–3.53 (m, 2H, CH₂). ¹³C NMR (CDCl₃ and MeOD): δ 160.9, 159.1, 150.1, 145.6, 130.4, 129.5, 126.9, 118.1, 116.7, 114.2, 110.4, 44.8, 36.9. HRMS (ES⁺) *m/z* found 337.0745; C₁₅H₁₃FN₂O₄S (M⁺ + H) requires 337.0658.

3-Iodophenyl-4-(2-oxoimidazolidin-1-yl)benzenesulfonate (38). Method B: flash chromatography (ethyl acetate to ethyl acetate/methanol 95:5). Yield: 80%. White solid. Mp: 182–184 °C. IR *v*: 3250, 2906, 1711 cm⁻¹. ¹H NMR (DMSO-*d*₆ and CDCl₃): δ 7.76–7.64 (m, 4H, Ar), 7.57 (d, 1H, J = 8.0 Hz, Ar), 7.34–7.32 (m, 1H, Ar), 7.25 (s, 1H,

NH), 7.04 (t, 1H, J = 8.0 Hz, Ar), 6.90–6.86 (m, 1H, Ar), 3.93–3.88 (m, 2H, CH₂), 3.52–3.47 (m, 2H, CH₂). ¹³C NMR (DMSO-*d*₆ and CDCl₃): δ 158.2, 149.3, 146.1, 135.8, 131.0, 129.1, 125.2, 121.4, 116.1, 93.5, 44.2, 36.4. HRMS (ES⁺) *m/z* found 444.9700; C₁₅H₁₃I-N₂O₄S (M⁺ + H) requires 444.9719.

3-Nitrophenyl-4-(2-oxoimidazolidin-1-yl)benzenesulfonate (39). Method B: flash chromatography (methylene chloride to methylene chloride/ethyl acetate 8:2). Yield: 98%. White solid. Mp: 152–153 °C. IR *v*: 3248, 1713 cm⁻¹. ¹H NMR (CDCl₃): δ 8.10–7.66 (m, 6H, Ar), 7.50–7.45 (m, 1H, Ar), 7.35–7.32 (m, 1H, Ar), 3.97–3.92 (m, 2H, CH₂), 3.63–3.57 (m, 2H, CH₂). ¹³C NMR (CDCl₃): δ 159.0, 149.7, 146.0, 130.5, 129.7, 128.9, 128.4, 126.3, 122.0, 118.0, 116.8, 44.8, 36.9. HRMS (ES⁺) *m/z* found 364.0343; C₁₅H₁₃N₃O₆S (M⁺ + H) requires 364.0603.

3-Aminophenyl-4-(2-oxoimidazolidin-1-yl)benzenesulfonate (40). Method C: flash chromatography (methylene chloride to methylene chloride/methanol 9:1). Yield: 32%. White solid. Mp: 184–185 °C. IR *v*: 3233, 1709 cm⁻¹. ¹H NMR (acetone-*d*₆): δ 7.87–7.73 (m, 4H, Ar), 6.96 (t, 1H, J = 8.1 Hz, Ar), 6.56–6.53 (m, 1H, Ar), 6.41–6.40 (m, 1H, Ar), 6.18–6.15 (m, 1H, Ar), 4.92 (s, 1H, NH), 4.04–4.00 (m, 2H, CH₂), 3.64–3.59 (m, 2H, CH₂). ¹³C NMR (acetone-*d*₆): δ 159.2, 150.8, 147.0, 130.4, 130.2, 130.0, 117.0, 117.0, 113.5, 110.2, 108.4, 45.3, 37.4. HRMS (ES⁺) *m/z* found 334.0578; C₁₅H₁₅N₃O₄S (M⁺ + H) requires 334.0862.

3,5-Dimethylphenyl-4-(2-oxoimidazolidin-1-yl)benzenesulfonate (41). Method B: flash chromatography (ethyl acetate to ethyl acetate/methanol 95:5). Yield: 75%. White solid. Mp: 200–203 °C. IR *v*: 3230, 1711 cm⁻¹. ¹H NMR (DMSO-*d*₆): δ 7.83–7.75 (m, 4H, Ar), 7.41 (s, 1H, Ar or NH), 6.95 (s, 1H, Ar or NH), 6.65 (s, 2H, Ar or NH), 3.95–3.89 (m, 2H, CH₂), 3.48–3.43 (m, 2H, CH₂), 2.21 (s, 6H, 2 × CH₃). ¹³C NMR (DMSO-*d*₆): δ 158.2, 149.1, 146.1, 139.4, 129.3, 128.7, 125.6, 119.4, 116.3, 44.3, 36.3, 20.7. HRMS (ES⁺) *m/z* found 347.0825; C₁₇H₁₈N₂O₄S (M⁺ + H) requires 347.1066.

3,4,5-Trimethylphenyl-4-(2-oxoimidazolidin-1-yl)benzenesulfonate (42). Method B: flash chromatography (methylene chloride to methylene chloride/ethyl acetate 0:1 to ethyl acetate/methanol 95:5). Yield: 79%. White solid. Mp: 211–212 °C. IR *v*: 3223, 2910, 1713 cm⁻¹. ¹H NMR (DMSO-*d*₆): δ 7.83–7.75 (m, 4H, Ar), 7.42 (s, 1H, NH), 6.67 (s, 2H, Ar), 3.95–3.90 (m, 2H, CH₂), 3.49–3.44 (m, 2H, CH₂), 2.17 (s, 6H, 2 × CH₃), 2.07 (s, 3H, CH₃). ¹³C NMR (DMSO-*d*₆): δ 158.3, 146.4, 146.0, 137.8, 134.0, 129.3, 125.8, 120.4, 116.3, 44.3, 36.3, 20.2, 14.7. HRMS (ES⁺) *m/z* found 361.1224; C₁₈H₂₀N₂O₄S (M⁺ + H) requires 361.1222.

3,4-Dimethoxyphenyl-4-(2-oxoimidazolidin-1-yl)benzenesulfonate (43). Method B: flash chromatography (methylene chloride to methylene chloride/ethyl acetate 0:1). Yield: 70%. White solid. Mp: 156–158 °C. IR *v*: 3235, 2969, 1710 cm⁻¹. ¹H NMR (CDCl₃ and MeOD): δ 7.66–7.58 (m, 4H, Ar), 6.63–6.60 (m, 1H, Ar), 6.48–6.47 (m, 1H, Ar), 6.38–6.34 (m, 1H, Ar), 3.90–3.85 (m, 2H, CH₂), 3.73 (s, 3H, CH₃), 3.66 (s, 3H, CH₃), 3.54–3.50 (m, 2H, CH₂), 3.32 (s, 1H, NH). ¹³C NMR (CDCl₃ and MeOD): δ 159.1, 149.2, 147.8, 145.4, 143.1, 129.6, 127.2, 116.6, 113.8, 110.9, 106.5, 56.0, 56.0, 44.8, 36.9. HRMS (ES⁺) *m/z* found 378.9391; C₁₇H₁₈N₂O₆S (M⁺ + H) requires 379.0964.

3,5-Dimethoxyphenyl-4-(2-oxoimidazolidin-1-yl)benzenesulfonate (44). Method B: flash chromatography (ethyl acetate to ethyl acetate/methanol 95:5). Yield: 71%. White solid. Mp: 219–221 °C. IR *v*: 3235, 1711 cm⁻¹. ¹H NMR (DMSO-*d*₆): δ 7.85–7.78 (m, 4H, Ar), 7.43 (s, 1H, NH), 6.46–6.45 (m, 1H, Ar), 6.18–6.17 (m, 2H, Ar), 3.95–3.90 (m, 2H, CH₂), 3.68 (s, 6H, 2 × CH₃), 3.49–3.44 (m, 2H, CH₂). ¹³C NMR (DMSO-*d*₆): δ 160.8, 158.2, 150.6, 146.2, 129.5, 125.3, 116.4, 100.6, 99.0, 55.6, 44.3, 36.3. HRMS (ES⁺) *m/z* found 379.0945; C₁₇H₁₈N₂O₆S (M⁺ + H) requires 379.0964.

3,4,5-Trimethoxyphenyl-4-(2-oxoimidazolidin-1-yl)benzenesulfonate (45). Method B: flash chromatography (methylene chloride to methylene chloride/ethyl acetate 7:3). Yield: 31%. Mp: 191–192 °C. IR ν : 3201, 1706 cm^{-1} . ^1H NMR (DMSO- d_6): δ 7.86–7.80 (m, 4H, Ar), 7.42 (s, 1H, NH), 6.31 (s, 2H, Ar), 3.95–3.90 (m, 2H, CH_2), 3.65 (s, 6H, 2 \times CH_3), 3.63 (s, 3H, CH_3), 3.49–3.44 (m, 2H, CH_2). ^{13}C NMR (DMSO- d_6): δ 158.2, 153.1, 146.2, 145.1, 136.3, 129.6, 125.2, 116.4, 100.0, 60.1, 56.1, 44.3, 36.2. HRMS (ES+) m/z found 409.1068; $\text{C}_{18}\text{H}_{20}\text{N}_2\text{O}_7\text{S}$ (M^+ + H) requires 409.1070.

3,5-Dichlorophenyl-4-(2-oxoimidazolidin-1-yl)benzenesulfonate (46). Method B: flash chromatography (ethyl acetate to ethyl acetate/methanol 95:5). Yield: 64%. White solid. Mp: 179–181 °C. IR ν : 3236, 1709 cm^{-1} . ^1H NMR (DMSO- d_6): δ 7.87–7.80 (m, 4H, Ar), 7.66 (m, 1H, Ar), 7.46 (s, 1H, NH), 7.21–7.20 (m, 2H, Ar), 3.97–3.91 (m, 2H, CH_2), 3.49–3.44 (m, 2H, CH_2). ^{13}C NMR (DMSO- d_6): δ 158.2, 149.7, 146.6, 134.7, 129.6, 127.6, 124.3, 121.7, 116.4, 44.2, 36.3. HRMS (ES+) m/z found 386.9956; $\text{C}_{15}\text{H}_{12}\text{Cl}_2\text{N}_2\text{O}_4\text{S}$ (M^+ + H) requires 386.9973.

3,4-Difluorophenyl-4-(2-oxoimidazolidin-1-yl)benzenesulfonate (47). Method B: flash chromatography (ethyl acetate to ethyl acetate/methanol 95:5). Yield: 78%. White solid. Mp: 182–184 °C. IR ν : 3230, 2918, 1716 cm^{-1} . ^1H NMR (DMSO- d_6 and CDCl_3): δ 7.77–7.51 (m, 5H, Ar and NH), 7.27–7.18 (m, 1H, Ar), 7.03–6.96 (m, 1H, Ar), 6.77–6.72 (m, 1H, Ar), 3.93–3.83 (m, 2H, CH_2), 3.51–3.43 (m, 2H, CH_2). ^{13}C NMR (DMSO- d_6 and CDCl_3): δ 158.8, 158.1, 146.2, 141.6, 138.9, 129.2, 126.2, 124.8, 118.8, 118.8, 118.7, 118.7, 117.7, 117.5, 116.2, 115.8, 112.4, 112.1, 44.5, 44.2, 36.6, 36.4. HRMS (ES+) m/z found 354.9966; $\text{C}_{15}\text{H}_{12}\text{F}_2\text{N}_2\text{O}_4\text{S}$ (M^+ + H) requires 355.0564.

3,5-Difluorophenyl-4-(2-oxoimidazolidin-1-yl)benzenesulfonate (48). Method B: flash chromatography (ethyl acetate to ethyl acetate/methanol 95:5). Yield: 90%. White solid. Mp: 172–174 °C. IR ν : 3225, 1716 cm^{-1} . ^1H NMR (DMSO- d_6 and CDCl_3): δ 7.75–7.66 (m, 4H, Ar), 7.07 (s, 1H, NH), 6.81–6.74 (m, 1H, Ar), 6.59–6.55 (m, 2H, Ar), 3.93–3.87 (m, 2H, CH_2), 3.54–3.48 (m, 2H, CH_2). ^{13}C NMR (DMSO- d_6 and CDCl_3): δ 164.0, 163.8, 160.7, 160.5, 158.2, 150.2, 146.1, 129.1, 125.0, 116.1, 106.4, 106.3, 106.1, 106.0, 103.0, 102.7, 102.3, 44.2, 36.4. HRMS (ES+) m/z found 355.0141; $\text{C}_{15}\text{H}_{12}\text{F}_2\text{N}_2\text{O}_4\text{S}$ (M^+ + H) requires 355.0564.

3,4,5-Trifluorophenyl-4-(2-oxoimidazolidin-1-yl)benzenesulfonate (49). Method B: flash chromatography (ethyl acetate to ethyl acetate/methanol 95:5). Yield: 99%. White solid. Mp: 178–180 °C. IR ν : 3238, 2914, 1714 cm^{-1} . ^1H NMR (DMSO- d_6 and CDCl_3): δ 7.78–7.67 (m, 4H, Ar), 7.24 (s, 1H, NH), 6.84–6.77 (m, 2H, Ar), 3.94–3.89 (m, 2H, CH_2), 3.53–3.48 (m, 2H, CH_2). ^{13}C NMR (DMSO- d_6 and CDCl_3): δ 158.1, 152.0, 151.9, 151.9, 151.8, 148.7, 148.6, 148.5, 148.5, 146.4, 143.8, 143.8, 143.7, 140.3, 140.1, 139.9, 136.8, 129.2, 124.5, 116.2, 108.0, 107.9, 107.8, 107.7, 44.2, 36.4. HRMS (ES+) m/z found 372.9821; $\text{C}_{15}\text{H}_9\text{F}_3\text{N}_2\text{O}_4\text{S}$ (M^+ + H) requires 373.0470.

3-Methyl-4-nitrophenyl-4-(2-oxoimidazolidin-1-yl)benzenesulfonate (50). Method B: flash chromatography (methylene chloride to methylene chloride/ethyl acetate 8:2). Yield: 65%. White solid. Mp: 215–216 °C. IR ν : 3225, 1713 cm^{-1} . ^1H NMR (DMSO- d_6): δ 8.03 (d, 1H, $J = 8.9$ Hz, Ar), 7.85–7.81 (m, 4H, Ar), 7.45 (s, 1H, NH), 7.32–7.31 (m, 1H, Ar), 7.10–7.07 (m, 1H, Ar), 3.95–3.90 (m, 2H, CH_2), 3.48–3.43 (m, 2H, CH_2), 2.49 (s, 3H, CH_3). ^{13}C NMR (DMSO- d_6): δ 158.2, 151.5, 147.3, 146.5, 135.7, 129.5, 126.7, 126.0, 124.7, 120.6, 116.5, 44.2, 36.3, 19.5. HRMS (ES+) m/z found 378.0916; $\text{C}_{16}\text{H}_{15}\text{N}_3\text{O}_6\text{S}$ (M^+ + H) requires 378.0760.

4-Amino-3-methylphenyl-4-(2-oxoimidazolidin-1-yl)benzenesulfonate (51). Method C: flash chromatography (methylene chloride to methylene chloride/methanol 9:1). Yield: 31%. yellow solid. Mp: 160–162 °C. IR ν : 3228, 1709 cm^{-1} . ^1H NMR (acetone- d_6): δ 7.87–7.70 (m, 4H, Ar), 6.75–6.69 (m, 1H, Ar), 6.57–6.37 (m, 2H,

Ar), 4.55 (s, 1H, NH), 4.06–4.00 (m, 2H, CH_2), 3.65–3.59 (m, 2H, CH_2), 1.29 (s, 3H, CH_3). ^{13}C NMR (acetone- d_6): δ 159.1, 146.9, 146.0, 141.4, 130.1, 124.6, 124.5, 120.9, 120.7, 116.9, 114.8, 45.3, 37.4, 17.4. HRMS (ES+) m/z found 348.1060; $\text{C}_{16}\text{H}_{17}\text{N}_3\text{O}_4\text{S}$ (M^+ + H) requires 348.1018.

4-Ethylphenyl-4-(2-oxoimidazolidin-1-yl)benzenesulfonate (52). Method B: flash chromatography (ethyl acetate to ethyl acetate/methanol 95:5). Yield: 79%. White solid. Mp: 155–157 °C. IR ν : 3230, 1715 cm^{-1} . ^1H NMR (DMSO- d_6): δ 7.83–7.74 (m, 4H, Ar), 7.42 (s, 1H, NH), 7.21 (d, 2H, $J = 8.4$ Hz, Ar), 6.92 (d, 2H, $J = 8.4$ Hz, Ar), 3.95–3.90 (m, 2H, CH_2), 3.49–3.43 (m, 2H, CH_2), 2.58 (q, 2H, $J = 7.5$ Hz, CH_2), 1.15 (t, 3H, $J = 7.5$ Hz, CH_3). ^{13}C NMR (DMSO- d_6): δ 158.2, 147.2, 146.1, 142.9, 129.4, 129.2, 125.4, 121.9, 116.3, 44.2, 36.3, 27.5, 15.4. HRMS (ES+) m/z found 347.0906; $\text{C}_{17}\text{H}_{18}\text{N}_2\text{O}_4\text{S}$ (M^+ + H) requires 347.1066.

4-Propylphenyl-4-(2-oxoimidazolidin-1-yl)benzenesulfonate (53). Method B: flash chromatography (ethyl acetate to ethyl acetate/methanol 95:5). Yield: 78%. White solid. Mp: 198–200 °C. IR ν : 3208, 2955, 1712 cm^{-1} . ^1H NMR (DMSO- d_6 and CDCl_3): δ 7.68–7.60 (m, 4H, Ar), 7.02 (s, 1H, Ar or NH), 6.99 (s, 1H, Ar or NH), 6.79–6.76 (m, 3H, Ar), 3.91–3.86 (m, 2H, CH_2), 3.54–3.49 (m, 2H, CH_2), 2.47 (t, 2H, $J = 7.6$ Hz, CH_2), 1.59–1.47 (m, 2H, CH_2), 0.84 (t, 3H, $J = 7.3$ Hz, CH_3). ^{13}C NMR (DMSO- d_6 and CDCl_3): δ 158.3, 147.1, 145.4, 141.2, 129.0, 129.0, 126.3, 121.5, 116.0, 44.2, 36.8, 36.5, 23.8, 13.3. HRMS (ES+) m/z found 361.0652; $\text{C}_{18}\text{H}_{20}\text{N}_2\text{O}_4\text{S}$ (M^+ + H) requires 361.1222.

4-sec-Butylphenyl-4-(2-oxoimidazolidin-1-yl)benzenesulfonate (54). Method B: flash chromatography (methylene chloride to methylene chloride/ethyl acetate 8:2). Yield: 74%. White solid. Mp: 179–180 °C. IR ν : 3245, 1711 cm^{-1} . ^1H NMR (acetone- d_6): δ 7.90–7.73 (m, 4H, Ar), 7.19 (d, 2H, $J = 8.6$ Hz, Ar), 6.95 (d, 2H, $J = 8.6$ Hz, Ar), 6.40 (brs, 1H, NH), 4.06–4.01 (m, 2H, CH_2), 3.65–3.60 (m, 2H, CH_2), 2.65–2.58 (m, 1H, CH), 1.58–1.23 (m, 2H, CH_2), 1.18 (d, 3H, $J = 6.9$ Hz, CH_3), 0.77 (t, 3H, $J = 7.4$ Hz, CH_3). ^{13}C NMR (acetone- d_6): δ 159.0, 147.6, 146.6, 145.3, 129.7, 128.1, 127.9, 122.1, 116.6, 44.9, 41.1, 37.1, 31.1, 21.7, 12.1. HRMS (ES+) m/z found 375.0776; $\text{C}_{19}\text{H}_{22}\text{N}_2\text{O}_4\text{S}$ (M^+ + H) requires 375.1379.

4-Ethoxyphenyl-4-(2-oxoimidazolidin-1-yl)benzenesulfonate (55). Method B: flash chromatography (ethyl acetate to ethyl acetate/methanol 95:5). Yield: 76%. White solid. Mp: 185–187 °C. IR ν : 3236, 2908, 1710 cm^{-1} . ^1H NMR (DMSO- d_6 and CDCl_3): δ 7.70–7.58 (m, 4H, Ar), 7.01 (s, 1H, NH), 6.79–6.75 (m, 2H, Ar), 6.72–6.68 (m, 2H, Ar), 3.95–3.86 (m, 4H, 2 \times CH_2), 3.53–3.48 (m, 2H, CH_2), 1.32 (t, 3H, $J = 7.0$ Hz, CH_3). ^{13}C NMR (DMSO- d_6 and CDCl_3): δ 158.3, 157.1, 145.6, 142.4, 129.0, 125.9, 122.9, 115.9, 114.6, 63.3, 44.2, 36.5, 14.4. HRMS (ES+) m/z found 363.0692; $\text{C}_{17}\text{H}_{18}\text{N}_2\text{O}_5\text{S}$ (M^+ + H) requires 363.1015.

4-Propoxyphenyl-4-(2-oxoimidazolidin-1-yl)benzenesulfonate (56). Method B: flash chromatography (methylene chloride to methylene chloride/ethyl acetate 8:2). Yield: 56%. White solid. Mp: 156–157 °C. IR ν : 3226, 1711 cm^{-1} . ^1H NMR (CDCl_3): δ 7.74–7.65 (m, 4H, Ar), 6.87–6.83 (m, 2H, Ar), 6.76–6.72 (m, 2H, Ar), 5.73 (s, 1H, NH), 3.98–3.93 (m, 2H, CH_2), 3.84 (t, 2H, $J = 6.5$ Hz, CH_2), 3.66–3.60 (m, 2H, CH_2), 1.80–1.71 (m, 2H, CH_2), 1.00 (t, 3H, $J = 7.4$ Hz, CH_3). ^{13}C NMR (CDCl_3): δ 158.9, 157.8, 145.3, 142.9, 129.7, 127.6, 123.3, 116.6, 115.0, 69.9, 44.9, 37.1, 22.5, 10.5. HRMS (ES+) m/z found 377.0320; $\text{C}_{18}\text{H}_{20}\text{N}_2\text{O}_5\text{S}$ (M^+ + H) requires 377.1171.

4-Butoxyphenyl-4-(2-oxoimidazolidin-1-yl)benzenesulfonate (57). Method B: flash chromatography (methylene chloride to methylene chloride/ethyl acetate 8:2). Yield: 58%. White solid. Mp: 151–152 °C. IR ν : 3218, 1696 cm^{-1} . ^1H NMR (CDCl_3): δ 7.67–7.59 (m, 4H, Ar), 6.80–6.76 (m, 2H, Ar), 6.70–6.66 (m, 2H, Ar), 3.92–3.80 (m, 4H, 2 \times CH_2), 3.57–3.52 (m, 2H, CH_2), 3.10 (s, 1H, NH), 1.70–1.61 (m, 2H, CH_2), 1.45–1.35 (m, 2H, CH_2), 0.88 (t, 3H,

$J = 7.4$ Hz, CH_3). ^{13}C NMR (CDCl_3): δ 159.2, 157.8, 145.3, 142.8, 129.6, 127.3, 123.2, 116.6, 115.0, 68.1, 44.8, 36.9, 31.1, 19.1, 13.7. HRMS (ES^+) m/z found 391.0821; $\text{C}_{19}\text{H}_{22}\text{N}_2\text{O}_5\text{S}$ ($\text{M}^+ + \text{H}$) requires 391.1328.

4-(tert-Butyldimethylsilyloxy)-4-(2-oxoimidazolidin-1-yl)benzenesulfonate (58). Method B: flash chromatography (methylene chloride to methylene chloride/ethyl acetate 3:1). Yield: 53%. White solid. Mp: 222–223 °C. IR ν : 3227, 1716 cm^{-1} . ^1H NMR (CDCl_3): δ 7.75–7.66 (m, 4H, Ar), 6.83–6.80 (m, 2H, Ar), 6.70–6.68 (m, 2H, Ar), 5.10 (s, 1H, NH), 4.00–3.95 (m, 2H, CH_2), 3.67–3.62 (m, 2H, CH_2), 0.95 (s, 9H, 3 \times CH_3), 0.16 (s, 6H, 2 \times CH_3). ^{13}C NMR (CDCl_3): δ 158.6, 154.4, 145.2, 143.6, 129.8, 127.7, 123.4, 120.7, 116.6, 44.9, 37.1, 25.6, 18.2, –4.5. HRMS (ES^+) m/z found 449.1561; $\text{C}_{21}\text{H}_{28}\text{N}_2\text{O}_5\text{SSi}$ ($\text{M}^+ + \text{H}$) requires 449.1567.

4-Chlorophenyl-4-(2-oxoimidazolidin-1-yl)benzenesulfonate (59). Method B: flash chromatography (methylene chloride to methylene chloride/ethyl acetate 8:2). Yield: 89%. White solid. Mp: 179–180 °C. IR ν : 3229, 1712 cm^{-1} . ^1H NMR ($\text{DMSO}-d_6$): δ 7.84–7.75 (m, 4H, Ar), 7.51–7.46 (m, 3H, Ar and NH), 7.07–7.04 (m, 2H, Ar), 3.95–3.90 (m, 2H, CH_2), 3.49–3.44 (m, 2H, CH_2). ^{13}C NMR ($\text{DMSO}-d_6$): δ 158.2, 131.7, 130.0, 129.5, 124.7, 124.1, 116.4, 115.6, 110.6, 44.2, 36.3. HRMS (ES^+) m/z found 353.0836; $\text{C}_{15}\text{H}_{13}\text{ClN}_2\text{O}_4\text{S}$ ($\text{M}^+ + \text{H}$) requires 353.0363.

4-Fluorophenyl-4-(2-oxoimidazolidin-1-yl)benzenesulfonate (60). Method B: flash chromatography (methylene chloride to methylene chloride/ethyl acetate 8:2). Yield: 33%. White solid. Mp: 208–209 °C. IR ν : 3227, 1714 cm^{-1} . ^1H NMR (CDCl_3 and MeOD): δ 7.65–7.58 (m, 4H, Ar), 6.90–6.83 (m, 4H, Ar), 3.91–3.86 (m, 2H, CH_2), 3.55–3.49 (m, 2H, CH_2). ^{13}C NMR (CDCl_3 and MeOD): δ 159.1, 145.5, 129.6, 126.8, 124.0, 123.9, 116.6, 116.4, 116.1, 44.8, 36.8. HRMS (ES^+) m/z found 337.0647; $\text{C}_{15}\text{H}_{13}\text{FN}_2\text{O}_4\text{S}$ ($\text{M}^+ + \text{H}$) requires 337.0658.

4-Iodophenyl-4-(2-oxoimidazolidin-1-yl)benzenesulfonate (61). Method B: flash chromatography (ethyl acetate to ethyl acetate/methanol 95:5). Yield: 74%. White solid. Mp: 202–204 °C. IR ν : 3203, 1710 cm^{-1} . ^1H NMR ($\text{DMSO}-d_6$ and CDCl_3): δ 7.73–7.70 (m, 2H, Ar), 7.64–7.55 (m, 4H, Ar), 7.13 (brs, 1H, NH), 6.71–6.68 (m, 2H, Ar), 3.92–3.87 (m, 2H, CH_2), 3.53–3.47 (m, 2H, CH_2). ^{13}C NMR ($\text{DMSO}-d_6$ and CDCl_3): δ 158.2, 149.0, 145.9, 138.3, 129.1, 125.4, 124.2, 116.1, 91.5, 44.2, 36.4. HRMS (ES^+) m/z found 444.9747; $\text{C}_{15}\text{H}_{13}\text{IN}_2\text{O}_4\text{S}$ ($\text{M}^+ + \text{H}$) requires 444.9719.

4-Nitrophenyl-4-(2-oxoimidazolidin-1-yl)benzenesulfonate (62). Method B: flash chromatography (methylene chloride to methylene chloride/ethyl acetate 7:3). Yield: 98%. White solid. Mp: 195–196 °C. IR ν : 3267, 1704 cm^{-1} . ^1H NMR ($\text{DMSO}-d_6$): δ 8.29 (d, 2H, $J = 9.1$ Hz, Ar), 7.83 (s, 4H, Ar), 7.46 (s, 1H, NH), 7.35 (d, 2H, $J = 9.1$ Hz, Ar), 3.96–3.91 (m, 2H, CH_2), 3.49–3.44 (m, 2H, CH_2). ^{13}C NMR ($\text{DMSO}-d_6$): δ 158.2, 153.4, 146.6, 146.0, 129.6, 125.8, 124.5, 123.4, 116.5, 44.2, 36.3. HRMS (ES^+) m/z found 363.9860; $\text{C}_{15}\text{H}_{13}\text{N}_3\text{O}_6\text{S}$ ($\text{M}^+ + \text{H}$) requires 364.0603.

4-Aminophenyl-4-(2-oxoimidazolidin-1-yl)benzenesulfonate (63). Method C: flash chromatography (methylene chloride to methylene chloride/methanol 9:1). Yield: 46%. White solid. Mp: 152–154 °C. IR ν : 3265, 1716 cm^{-1} . ^1H NMR ($\text{DMSO}-d_6$): δ 7.81–7.68 (m, 4H, Ar), 7.40 (s, 1H, Ar), 6.78–6.76 (m, 1H, Ar), 6.62 (d, 1H, $J = 8.7$ Hz, Ar), 6.44 (d, 1H, $J = 8.7$ Hz, Ar), 5.20 (s, 1H, NH), 3.95–3.90 (m, 2H, CH_2), 3.48–3.41 (m, 2H, CH_2). ^{13}C NMR ($\text{DMSO}-d_6$): δ 158.3, 145.9, 139.1, 129.4, 122.6, 122.3, 116.2, 114.0, 113.3, 44.3, 36.3. HRMS (ES^+) m/z found 333.9906; $\text{C}_{15}\text{H}_{15}\text{N}_3\text{O}_4\text{S}$ ($\text{M}^+ + \text{H}$) requires 334.0862.

2-Methylquinolin-8-yl-4-(2-oxoimidazolidin-1-yl)benzenesulfonate (64). Method B: flash chromatography (methylene chloride to methylene chloride/methanol 9:1). Yield: 82%. Mp: 234–235 °C. IR ν : 3255, 1724 cm^{-1} . ^1H NMR ($\text{DMSO}-d_6$): δ 8.25 (d, 1H, $J = 8.4$ Hz, Ar), 7.91–7.87 (m, 1H, Ar), 7.82–7.69 (m, 4H, Ar), 7.58–7.51 (m, 2H,

Ar), 7.41 (d, 1H, $J = 8.4$ Hz, Ar), 7.36 (s, 1H, NH), 3.89–3.84 (m, 2H, CH_2), 3.47–3.41 (m, 2H, CH_2), 2.53 (s, 3H, CH_3). ^{13}C NMR ($\text{DMSO}-d_6$): δ 159.5, 158.2, 145.9, 144.3, 140.2, 136.0, 129.6, 127.7, 127.2, 126.4, 125.3, 123.0, 122.6, 115.8, 44.3, 36.3, 24.9. HRMS (ES^+) m/z found 384.0133; $\text{C}_{19}\text{H}_{17}\text{N}_3\text{O}_4\text{S}$ ($\text{M}^+ + \text{H}$) requires 384.1018.

1H-Indol-5-yl-4-(2-oxoimidazolidin-1-yl)benzenesulfonate (65). Method B: flash chromatography (methylene chloride to methylene chloride/ethyl acetate 7:3). Yield: 82%. White solid. Mp: 226–227 °C. IR ν : 3417, 1712 cm^{-1} . ^1H NMR ($\text{DMSO}-d_6$): δ 11.28 (s, 1H, NH), 7.80–7.71 (m, 4H, Ar), 7.43–7.39 (m, 2H, Ar), 7.33–7.30 (m, 1H, Ar), 7.21–7.20 (m, 1H, Ar), 6.70–6.66 (m, 1H, Ar), 6.43 (brs, 1H, NH), 3.93–3.88 (m, 2H, CH_2), 3.47–3.42 (m, 2H, CH_2). ^{13}C NMR ($\text{DMSO}-d_6$): δ 158.3, 145.9, 142.5, 134.2, 129.3, 127.6, 127.4, 125.8, 116.3, 115.2, 112.9, 112.0, 101.7, 44.2, 36.3. HRMS (ES^+) m/z found 358.0028; $\text{C}_{17}\text{H}_{15}\text{N}_3\text{O}_4\text{S}$ ($\text{M}^+ + \text{H}$) requires 358.0862.

Pyridin-2-yl-4-(2-oxoimidazolidin-1-yl)benzenesulfonate (66). Method B: not washed with hydrochloric acid; flash chromatography (methylene chloride to methylene chloride/ethyl acetate 0:1). Yield: 32%. White solid. Mp: 153–155 °C. IR ν : 3228, 3117, 1695 cm^{-1} . ^1H NMR ($\text{DMSO}-d_6$): δ 8.31–8.29 (m, 1H, Ar), 8.00–7.95 (m, 1H, Ar), 7.89–7.81 (m, 4H, Ar), 7.53–7.39 (m, 2H, NH and Ar), 7.20–7.17 (m, 1H, Ar), 3.96–3.91 (m, 2H, CH_2), 3.49–3.44 (m, 2H, CH_2). ^{13}C NMR ($\text{DMSO}-d_6$): δ 158.2, 156.4, 148.4, 146.1, 141.1, 129.4, 126.8, 123.4, 116.3, 115.8, 44.3, 36.3. HRMS (ES^+) m/z found 320.0730; $\text{C}_{14}\text{H}_{13}\text{N}_3\text{O}_4\text{S}$ ($\text{M}^+ + \text{H}$) requires 320.0705.

Pyridin-4-yl-4-(2-oxoimidazolidin-1-yl)benzenesulfonate (67). Method B: not washed with hydrochloric acid; flash chromatography (methylene chloride to methylene chloride/methanol 9:1). Yield: 28%. White solid. Mp: 188–192 °C. IR ν : 3226, 3114, 1729 cm^{-1} . ^1H NMR ($\text{DMSO}-d_6$): δ 8.59 (d, 2H, $J = 7.0$ Hz, Ar), 7.56–7.49 (m, 4H, Ar), 7.27 (d, 2H, $J = 7.0$ Hz, Ar), 7.00 (s, 1H, NH), 3.88–3.83 (m, 2H, CH_2), 3.44–3.39 (m, 2H, CH_2). ^{13}C NMR ($\text{DMSO}-d_6$): δ 171.6, 158.9, 143.0, 141.4, 140.8, 126.0, 115.7, 114.0, 44.5, 36.5. HRMS (ES^+) m/z found 320.0730; $\text{C}_{14}\text{H}_{13}\text{N}_3\text{O}_4\text{S}$ ($\text{M}^+ + \text{H}$) requires 320.0705.

4-(1H-Imidazol-1-yl)phenyl-4-(2-oxoimidazolidin-1-yl)benzenesulfonate (68). Method B: flash chromatography (ethyl acetate to ethyl acetate/methanol 9:1). Yield: 74%. White solid. Mp: 206–208 °C. IR ν : 3220, 2910, 2811, 1713 cm^{-1} . ^1H NMR ($\text{DMSO}-d_6$): δ 8.26 (s, 1H, Ar), 7.86–7.78 (m, 4H, Ar), 7.74 (s, 1H, Ar), 7.71 (s, 1H, Ar), 7.68 (s, 1H, Ar), 7.43 (brs, 1H, NH), 7.19 (s, 1H, Ar), 7.16 (s, 1H, Ar), 7.11 (s, 1H, Ar), 3.95–3.90 (m, 2H, CH_2), 3.49–3.44 (m, 2H, CH_2). ^{13}C NMR ($\text{DMSO}-d_6$): δ 158.2, 147.3, 146.3, 135.7, 130.1, 129.5, 125.0, 123.6, 121.7, 118.1, 116.4, 44.3, 36.3. HRMS (ES^+) m/z found 385.0567; $\text{C}_{18}\text{H}_{16}\text{N}_4\text{O}_4\text{S}$ ($\text{M}^+ + \text{H}$) requires 385.0971.

2-Tolyl-4-[tetrahydro-2-oxopyrimidin-1(2H)-yl]benzenesulfonate (69). Method B: flash chromatography (ethyl acetate to ethyl acetate/methanol 95:5). Yield: 58%. White solid. Mp: 161–163 °C. IR ν : 3209, 2944, 1657 cm^{-1} . ^1H NMR ($\text{DMSO}-d_6$): δ 7.81–7.65 (m, 4H, Ar), 7.32–7.22 (m, 3H, Ar and NH), 7.03–7.00 (m, 2H, Ar), 3.76–3.72 (m, 2H, CH_2), 3.27–3.23 (m, 2H, CH_2), 2.07 (s, 3H, CH_3), 2.03–1.98 (m, 2H, CH_2). ^{13}C NMR ($\text{DMSO}-d_6$): δ 153.7, 149.7, 147.8, 131.8, 131.0, 128.3, 128.3, 127.4, 127.3, 123.5, 121.9, 47.1, 39.7, 22.0, 15.9. HRMS (ES^+) m/z found 347.1064; $\text{C}_{17}\text{H}_{18}\text{N}_2\text{O}_4\text{S}$ ($\text{M}^+ + \text{H}$) requires 347.1065.

2-Ethylphenyl-4-[tetrahydro-2-oxopyrimidin-1(2H)-yl]benzenesulfonate (70). Method B: flash chromatography (ethyl acetate to ethyl acetate/methanol 95:5). Yield: 69%. White solid. Mp: 142–144 °C. IR ν : 3209, 2976, 1655 cm^{-1} . ^1H NMR ($\text{DMSO}-d_6$): δ 7.83–7.66 (m, 4H, Ar), 7.37–7.22 (m, 3H, Ar), 7.03–7.00 (m, 2H, Ar and NH), 3.74 (t, 2H, $J = 5.7$ Hz, CH_2), 3.27–3.24 (m, 2H, CH_2), 2.49 (q, 2H, $J = 7.5$ Hz, CH_2), 2.00 (quint, 2H, $J = 5.7$ Hz, CH_2), 1.07 (t, 3H, $J = 7.5$ Hz, CH_3). ^{13}C NMR ($\text{DMSO}-d_6$): δ 153.7, 149.7, 147.3, 136.7, 130.2, 128.4, 128.2, 127.4, 127.3, 123.5, 121.7, 47.1, 39.7, 22.2, 22.0, 14.1. HRMS (ES^+) m/z found 361.1223; $\text{C}_{18}\text{H}_{20}\text{N}_2\text{O}_4\text{S}$ ($\text{M}^+ + \text{H}$) requires 361.1222.

2-Propylphenyl-4-[tetrahydro-2-oxopyrimidin-1(2H)-yl]benzenesulfonate (71). Method B: flash chromatography (methylene chloride to methylene chloride/methanol 9:1). Yield: 98%. White solid. Mp: 131–132 °C. IR ν : 3223, 1955, 1667 cm^{-1} . ^1H NMR (DMSO- d_6): δ 7.81–7.65 (m, 4H, Ar), 7.33–7.21 (m, 3H, Ar and NH), 7.04–7.01 (m, 2H, Ar), 3.73 (t, 2H, J = 5.6 Hz, CH_2), 3.26–3.23 (m, 2H, CH_2), 2.42–2.38 (m, 2H, CH_2), 1.98 (quint, 2H, J = 5.6 Hz, CH_2), 1.48–1.41 (m, 2H, CH_2), 0.82 (t, 3H, J = 7.3 Hz, CH_3). ^{13}C NMR (DMSO- d_6): δ 153.7, 149.7, 147.6, 135.1, 130.8, 128.5, 128.2, 127.4, 127.3, 123.5, 121.8, 47.1, 39.7, 31.2, 22.6, 22.0, 13.8. HRMS (ES+) m/z found 375.1172; $\text{C}_{19}\text{H}_{22}\text{N}_2\text{O}_4\text{S}$ (M^+ + H) requires 375.1378.

2,4-Dimethylphenyl-4-[tetrahydro-2-oxopyrimidin-1(2H)-yl]benzenesulfonate (72). Method B: flash chromatography (ethyl acetate to ethyl acetate/methanol 95:5). Yield: 62%. White solid. Mp: 161–163 °C. IR ν : 3228, 2949, 1684 cm^{-1} . ^1H NMR (DMSO- d_6): δ 7.79–7.65 (m, 4H, Ar), 7.10 (s, 1H, NH), 7.03–7.02 (m, 2H, Ar), 6.88–6.86 (m, 1H, Ar), 3.74 (t, 2H, J = 5.6 Hz, CH_2), 3.27–3.24 (m, 2H, CH_2), 2.27 (s, 3H, CH_3), 2.01–1.96 (m, 5H, CH_2 and CH_3). ^{13}C NMR (DMSO- d_6): δ 153.7, 149.6, 145.7, 136.6, 132.2, 130.6, 128.4, 128.3, 127.7, 123.5, 121.7, 47.1, 39.7, 22.0, 20.3, 15.8. HRMS (ES+) m/z found 361.1222; $\text{C}_{18}\text{H}_{20}\text{N}_2\text{O}_4\text{S}$ (M^+ + H) requires 361.1222.

2,4,5-Trichlorophenyl-4-[tetrahydro-2-oxopyrimidin-1(2H)-yl]benzenesulfonate (73). Method B: flash chromatography (methylene chloride to methylene chloride/methanol 9:1). Yield: 88%. White solid. Mp: 199–201 °C. IR ν : 3221, 3094, 1673 cm^{-1} . ^1H NMR (DMSO- d_6): δ 8.05 (s, 1H, NH or Ar), 7.85–7.66 (m, 4H, Ar), 7.61 (s, 1H, NH or Ar), 7.04 (brs, 1H, NH or Ar), 3.74 (t, 2H, J = 5.6 Hz, CH_2), 3.26–3.23 (m, 2H, CH_2), 1.99 (quint, 2H, J = 5.6 Hz, CH_2). ^{13}C NMR (DMSO- d_6): δ 153.6, 150.3, 143.9, 131.7, 131.0, 130.7, 128.8, 126.8, 126.6, 125.7, 123.4, 47.0, 39.7, 22.0. HRMS (ES+) m/z found 434.9741; $\text{C}_{16}\text{H}_{13}\text{Cl}_3\text{N}_2\text{O}_4\text{S}$ (M^+ + H) requires 434.9740.

2,4,6-Trichlorophenyl-4-[tetrahydro-2-oxopyrimidin-1(2H)-yl]benzenesulfonate (74). Method B: flash chromatography (ethyl acetate to ethyl acetate/methanol 95:5). Yield: 68%. White solid. Mp: 219–221 °C. IR ν : 3230, 3077, 1672 cm^{-1} . ^1H NMR (DMSO- d_6): δ 7.95–7.70 (m, 6H, Ar), 7.05 (s, 1H, NH), 3.77 (t, 2H, J = 5.6 Hz, CH_2), 3.28–3.25 (m, 2H, CH_2), 2.04–1.96 (m, 2H, CH_2). ^{13}C NMR (DMSO- d_6): δ 153.7, 150.2, 141.7, 132.5, 130.1, 129.6, 128.7, 128.6, 123.4, 47.1, 39.7, 22.0. HRMS (ES+) m/z found 434.9742; $\text{C}_{16}\text{H}_{13}\text{Cl}_3\text{N}_2\text{O}_4\text{S}$ (M^+ + H) requires 434.9740.

3-Tolyl-4-[tetrahydro-2-oxopyrimidin-1(2H)-yl]benzenesulfonate (75). Method B: flash chromatography (ethyl acetate to ethyl acetate/methanol 95:5). Yield: 57%. White solid. Mp: 145–147 °C. IR ν : 3209, 1675 cm^{-1} . ^1H NMR (DMSO- d_6): δ 7.79–7.63 (m, 4H, Ar), 7.30–7.14 (m, 2H, Ar), 7.01 (brs, 1H, NH), 6.93 (s, 1H, Ar), 6.83–6.81 (m, 1H, Ar), 3.75–3.72 (m, 2H, CH_2), 3.27–3.24 (m, 2H, CH_2), 2.29 (s, 3H, CH_3), 2.01–1.97 (m, 2H, CH_2). ^{13}C NMR (DMSO- d_6): δ 153.7, 149.6, 149.1, 140.0, 129.7, 128.4, 128.0, 127.8, 123.4, 122.5, 118.8, 47.0, 39.7, 22.0, 20.8. HRMS (ES+) m/z found 347.1066; $\text{C}_{17}\text{H}_{18}\text{N}_2\text{O}_4\text{S}$ (M^+ + H) requires 347.1065.

3-Methoxyphenyl-4-[tetrahydro-2-oxopyrimidin-1(2H)-yl]benzenesulfonate (76). Method B: flash chromatography (methylene chloride to methylene chloride/methanol 9:1). Yield: 72%. White solid. Mp: 132–134 °C. IR ν : 3218, 3081, 1667 cm^{-1} . ^1H NMR (DMSO- d_6): δ 7.79–7.62 (m, 4H, Ar), 7.33–7.27 (m, 1H, Ar), 7.01 (brs, 1H, NH), 6.91–6.88 (m, 1H, Ar), 6.64–6.62 (m, 1H, Ar), 6.57–6.56 (m, 1H, Ar), 3.72 (t, 2H, J = 5.8 Hz, CH_2), 3.68 (s, 3H, CH_3), 3.25–3.224 (m, 2H, CH_2), 1.99–1.96 (m, 2H, CH_2). ^{13}C NMR (DMSO- d_6): δ 160.1, 153.7, 150.0, 149.6, 130.5, 128.4, 127.6, 123.4, 113.9, 113.2, 107.9, 55.5, 47.0, 39.7, 22.0. HRMS (ES+) m/z found 363.1013; $\text{C}_{17}\text{H}_{18}\text{N}_2\text{O}_5\text{S}$ (M^+ + H) requires 363.1014.

3-Fluorophenyl-4-[tetrahydro-2-oxopyrimidin-1(2H)-yl]benzenesulfonate (77). Method B: flash chromatography (methylene chloride to methylene chloride/methanol 9:1). Yield: 74%. White solid.

Mp: 149–150 °C. IR ν : 3209, 3076, 1670 cm^{-1} . ^1H NMR (DMSO- d_6): δ 7.80–7.63 (m, 4H, Ar), 7.54–7.42 (m, 1H, Ar), 7.25–7.19 (m, 1H, Ar), 7.05–7.01 (m, 1H, Ar), 6.94–6.91 (m, 1H, Ar), 3.74–3.60 (m, 2H, CH_2), 3.24 (t, 2H, J = 5.7 Hz, CH_2), 1.97 (quint, 2H, J = 5.7 Hz, CH_2). ^{13}C NMR (DMSO- d_6): δ 153.7, 149.8, 131.5, 131.3, 128.5, 127.1, 125.5, 123.9, 123.4, 118.3, 118.3, 114.7, 114.4, 110.3, 110.0, 47.0, 22.1, 22.0. HRMS (ES+) m/z found 351.0816; $\text{C}_{16}\text{H}_{15}\text{FN}_2\text{O}_4\text{S}$ (M^+ + H) requires 351.0815.

3,4,5-Trimethoxyphenyl-4-[tetrahydro-2-oxopyrimidin-1(2H)-yl]benzenesulfonate (78). Method B: flash chromatography (methylene chloride to methylene chloride/ethyl acetate 7:3). Yield: 75%. White solid. Mp: 218–220 °C. IR ν : 3430, 1697 cm^{-1} . ^1H NMR (DMSO- d_6): δ 7.81–7.62 (m, 4H, Ar), 7.00 (brs, 1H, NH), 6.28 (s, 2H, Ar), 3.72 (t, 2H, J = 5.6 Hz, CH_2), 3.64 (s, 6H, $2 \times \text{CH}_3$), 3.63 (s, 3H, CH_3), 3.28–3.23 (m, 2H, CH_2), 2.02–1.95 (m, 2H, CH_2). ^{13}C NMR (DMSO- d_6): δ 153.7, 153.1, 149.8, 145.0, 136.3, 128.7, 127.6, 123.7, 100.0, 60.1, 56.1, 47.1, 39.7, 22.0. HRMS (ES+) m/z found 423.1227; $\text{C}_{19}\text{H}_{22}\text{N}_2\text{O}_7\text{S}$ (M^+ + H) requires 423.1226.

4-Tolyl-4-[tetrahydro-2-oxopyrimidin-1(2H)-yl]benzenesulfonate (79). Method B: flash chromatography (ethyl acetate to ethyl acetate/methanol 95:5). Yield: 72%. White solid. Mp: 204–205 °C. IR ν : 3213, 3067, 1667 cm^{-1} . ^1H NMR (DMSO- d_6): δ 7.77–7.63 (m, 4H, Ar), 7.21–7.18 (m, 2H, Ar), 7.02 (brs, 1H, NH), 6.95–6.92 (m, 2H, Ar), 3.74–3.71 (m, 2H, CH_2), 3.28–3.23 (m, 2H, CH_2), 2.29 (s, 3H, CH_3), 2.02–1.95 (m, 2H, CH_2). ^{13}C NMR (DMSO- d_6): δ 153.7, 149.5, 147.0, 136.9, 130.4, 128.4, 127.7, 123.3, 121.8, 47.0, 39.7, 22.0, 20.4. HRMS (ES+) m/z found 347.1063; $\text{C}_{17}\text{H}_{18}\text{N}_2\text{O}_4\text{S}$ (M^+ + H) requires 347.1065.

4-Chlorophenyl-4-[tetrahydro-2-oxopyrimidin-1(2H)-yl]benzenesulfonate (80). Method B: flash chromatography (ethyl acetate to ethyl acetate/methanol 95:5). Yield: 77%. White solid. Mp: 190–192 °C. IR ν : 3231, 3062, 1648 cm^{-1} . ^1H NMR (DMSO- d_6): δ 7.79–7.65 (m, 4H, Ar), 7.50–7.47 (m, 2H, Ar), 7.12–7.09 (m, 2H, Ar), 7.03 (brs, 1H, NH), 3.74 (t, 2H, J = 5.4 Hz, CH_2), 3.27–3.24 (m, 2H, CH_2), 2.03–1.96 (m, 2H, CH_2). ^{13}C NMR (DMSO- d_6): δ 153.7, 149.8, 147.8, 131.8, 130.1, 128.5, 127.1, 124.0, 123.3, 47.0, 39.7, 22.0. HRMS (ES+) m/z found 367.0529; $\text{C}_{16}\text{H}_{15}\text{ClN}_2\text{O}_4\text{S}$ (M^+ + H) requires 367.0519.

4-Fluorophenyl-4-[tetrahydro-2-oxopyrimidin-1(2H)-yl]benzenesulfonate (81). Method B: flash chromatography (ethyl acetate to ethyl acetate/methanol 95:5). Yield: 80%. White solid. Mp: 172–174 °C. IR ν : 3224, 3088, 1666 cm^{-1} . ^1H NMR (DMSO- d_6): δ 7.78–7.64 (m, 4H, Ar), 7.29–7.23 (m, 2H, Ar), 7.13–7.09 (m, 2H, Ar), 7.03 (s, 1H, NH), 3.75–3.72 (m, 2H, CH_2), 3.28–3.23 (m, 2H, CH_2), 2.02–1.97 (m, 2H, CH_2). ^{13}C NMR (DMSO- d_6): δ 153.7, 149.7, 145.2, 145.2, 128.5, 127.2, 124.2, 124.1, 123.3, 116.9, 116.6, 47.0, 39.7, 22.0. HRMS (ES+) m/z found 351.0814; $\text{C}_{16}\text{H}_{15}\text{FN}_2\text{O}_4\text{S}$ (M^+ + H) requires 351.0815.

General Procedure for the Synthesis of Compounds 82 and 83. 2-Chloroethyl isocyanate or 3-chloropropyl isocyanate (1.2 equiv) was added dropwise to a cold solution (ice bath) of the aniline (1.0 equiv) in dry methylene chloride (15 mL per g of aniline). The ice bath was then removed, and the reaction mixture was stirred at room temperature for 24 h. After completion of the reaction, the solvent was evaporated under reduced pressure to give white solid, which was triturated twice with cold hexanes/ether 10:1.

1-(2-Chloroethyl)-3-phenylurea (82). Yield: 99%. Mp: 108–110 °C. IR ν : 3304, 1637 cm^{-1} . ^1H NMR (DMSO- d_6): δ 8.69 (s, 1H, NH), 7.44–7.41 (m, 2H, Ar), 7.27–7.22 (m, 2H, Ar), 6.95–6.90 (m, 1H, Ar), 6.45 (t, 1H, J = 5.1 Hz, NH), 3.68 (t, 2H, J = 6.1 Hz, CH_2), 3.48–3.42 (m, 2H, CH_2). ^{13}C NMR (CDCl₃ and MeOD): δ 156.5, 138.9, 128.8, 122.7, 119.5, 44.0, 41.7.

1-(3-Chloropropyl)-3-phenylurea (83). Yield: 93%. Mp: 115–117 °C. IR ν : 3329, 1633 cm^{-1} . ^1H NMR (DMSO- d_6): δ 8.45 (s, 1H, NH), 7.43–7.40 (m, 2H, Ar), 7.26–7.21 (m, 2H, Ar), 6.93–6.88 (m,

1H, Ar), 6.27 (t, 1H, $J = 5.6$ Hz, NH), 3.68 (t, 2H, $J = 6.5$ Hz, CH₂), 3.27–3.21 (m, 2H, CH₂), 1.90 (apparent quint, 2H, $J = 6.5$ Hz, CH₂). ¹³C NMR (DMSO-*d*₆): δ 155.3, 140.5, 128.6, 121.1, 117.7, 43.1, 36.6, 32.7.

Preparation of Compounds 84 and 85. Sodium hydride (3 equiv) was added slowly to a cold solution of compound 82 or 83 (1 equiv) in tetrahydrofuran under dry nitrogen atmosphere. The ice bath was then removed after 30 min, and the reaction mixture was stirred at room temperature for 5 h. The reaction was quenched at 0 °C with water and diluted with ethyl acetate. The organic layer was washed with water and brine, dried over sodium sulfate, filtered, and concentrated in vacuo to afford 84 or 85 as white solids, which were used without further purification.

1-Phenylimidazolidin-2-one (84). Yield: 98%. Compound 84 was also synthesized using method described by Neville.⁴⁴ Briefly, triphosgene (12.2 mmol) was dissolved in 40 mL of tetrahydrofuran and cooled at 0 °C. To the resulting solution was added 36.7 mmol of *N*-phenylethylenediamine dissolved in 65 mL of tetrahydrofuran and 7.7 mL of triethylamine over a period of 30 min. A white solid immediately precipitated, and the reaction was complete after 5 min. The reaction mixture was quenched with water and diluted with ethyl acetate. The organic layer was washed with water and brine, dried over sodium sulfate, filtered, and concentrated in vacuo. The residue was purified by flash chromatography (methylene chloride to methylene chloride/ethyl acetate 3:10) to afford a white solid. Yield: 80%. Mp: 154–156 °C. IR ν : 3240, 1680 cm⁻¹. ¹H NMR (DMSO-*d*₆): δ 7.58–7.55 (m, 2H, Ar), 7.34–7.29 (m, 2H, Ar), 7.02–6.95 (m, 2H, Ar and NH), 3.88–3.83 (m, 2H, CH₂), 3.44–3.39 (m, 2H, CH₂). ¹³C NMR (CDCl₃): δ 160.2, 140.2, 128.8, 122.7, 117.9, 45.3, 37.5.

Tetrahydro-3-phenylpyrimidin-2(1H)-one (85). Yield: 95%. Mp: 198–200 °C. IR ν : 3216, 3060, 1643 cm⁻¹. ¹H NMR (DMSO-*d*₆): δ 7.32–7.28 (m, 4H, Ar), 7.14–7.10 (m, 1H, Ar), 6.58 (s, 1H, NH), 3.63 (t, 2H, $J = 5.7$ Hz, CH₂), 3.27–3.22 (m, 2H, CH₂), 1.96 (apparent quint, 2H, $J = 5.7$ Hz, CH₂). ¹³C NMR (DMSO-*d*₆): δ 154.4, 144.4, 128.1, 125.1, 124.2, 48.0, 22.2.

Preparation of Compounds 86 and 87. To 1.5 mL (23.1 mmol) of chlorosulfonic acid in 3 mL of carbon tetrachloride at 0 °C was added slowly (3.1 mmol) to compound 84 or 85. The reaction was almost completed after 2 h at 0 °C. The reaction mixture was poured slowly onto ice–water and filtered to collect the solid. The white solid was dried under vacuum.

4-(2-Oxoimidazolidin-1-yl)benzene-1-sulfonyl Chloride (86). Yield: 56%. Mp: 257–259 °C. IR ν : 3232, 1711 cm⁻¹. ¹H NMR (DMSO-*d*₆): δ 7.57–7.51 (m, 4H, Ar), 3.88–3.82 (m, 2H, CH₂), 3.44–3.38 (m, 2H, CH₂). ¹³C NMR (DMSO-*d*₆): δ 158.9, 141.2, 140.5, 126.1, 115.8, 44.5, 36.5.

4-(Tetrahydro-2-oxypyrimidin-1(2H)-yl)benzene-1-sulfonyl Chloride (87). Yield: 32%. Mp: 262–266 °C. IR ν : 3093, 1667 cm⁻¹. ¹H NMR (DMSO-*d*₆): δ 7.56 (d, 2H, $J = 8.3$ Hz, Ar), 7.28 (d, 2H, $J = 8.3$ Hz, Ar), 3.66–3.61 (m, 2H, CH₂), 3.41–3.23 (m, 2H, CH₂), 2.03–1.92 (m, 2H, CH₂). ¹³C NMR (DMSO-*d*₆): δ 154.6, 143.9, 143.8, 125.7, 124.4, 48.0, 21.7.

CoMFA and CoMSIA: Superimposition of PIB-SOs. All calculations were performed on SGI Onyx 3800 supercomputer system and Windows system. SYBYL molecular modeling software package was used to perform the QSAR analysis.⁶⁴ In CoMSIA studies, an sp³ carbon atom with a unit positive charge was used as a probe to evaluate five interaction fields: steric, electrostatic, hydrophobic, hydrogen bond donor, and hydrogen bond acceptor. All aligned molecules were set in a Cartesian coordinates box. The probe was used to calculate the field potentials in the box with a 2 Å grid resolution. In order to get an optimal QSAR models, other different descriptors were used to optimize the QSAR equation. Those descriptors involved in optimizing the QSAR analysis are molecular weight (MW), molecular volume (*V*), molar

refractivity (MR), polar volume (PV), polar surface area (PSA), log *P* value (Log*P*), and the similarity data of each compound to the hypothesis. An integer parameter was used to describe the five- and six-member rings of imidazolidinone and the adjacent phenyl moieties. In CoMFA studies, Tripos standard fields were used as CoMFA field classes and an sp³ carbon atom with a unit positive charge was used as the probe to evaluate steric and electrostatic potentials at every lattice point. The resolution of the grid was 2 Å. Distance method was used to control the form of the Coulombic electrostatic energy calculation. A 30 kcal/mol cutoff was used for steric and electrostatic field values. In addition to the CoMFA fields, all descriptors used in optimizing the CoMSIA models were also used in optimizing CoMFA models.

■ ASSOCIATED CONTENT

S Supporting Information. Synthesis, chemical characterization, and antiproliferative activity of compounds 88 and 89; predictive activities CoMSIA models A, B, and C and CoMFA models G, H, and I. This material is available free of charge via the Internet at <http://pubs.acs.org>.

■ AUTHOR INFORMATION

Corresponding Author

*For S.F.: phone, 418-525-4444, extension 52364; fax, 418-525-4372; e-mail, sebastien.fortin.1@ulaval.ca. For R.C.-G.: phone, 418-525-4444, extension 52363; fax, 418-525-4372; e-mail, rene.c-gaudreault@crsfa.ulaval.ca.

Present Addresses

[∞]Héma-Québec, 1070, Avenue des Sciences-dela-Vie, Québec, Québec, G1 V 5C3, Canada.

■ ACKNOWLEDGMENT

This work was supported by the Canadian Institutes of Health Research (R.C.-G, Grant MOP-79334 and Grant MOP-89707). S.F. is a recipient of a studentship from the Canadian Institutes of Health Research (Grant CGD-83623). We also acknowledge the technical expertise of Dr. Michel Déry for HPLC–MS experiments.

■ ABBREVIATIONS USED

PIB-SO, phenyl 4-(2-oxoimidazolidin-1-yl)benzenesulfonate; CEU, *N*-phenyl-*N'*-(2-chloroethyl)urea; CAM, chick chorioallantoic membrane tumor; PPB-SO, phenyl 4-(tetrahydro-2-oxypyrimidin-1(2H)-yl)benzenesulfonate; CoMFA, comparative molecular field analysis; CoMSIA, comparative molecular similarity indices analysis; C-BS, colchicine-binding site; EBI, *N,N'*-ethylenebis(iodoacetamide)

■ REFERENCES

- (1) Jordan, M. A.; Wilson, L. Microtubules as a target for anticancer drugs. *Nat. Rev. Cancer* **2004**, *4*, 253–265.
- (2) Teicher, B. A. Newer cytotoxic agents: attacking cancer broadly. *Clin. Cancer Res.* **2008**, *14*, 1610–1617.
- (3) Spencer, C. M.; Faulds, D. Paclitaxel. A review of its pharmacodynamic and pharmacokinetic properties and therapeutic potential in the treatment of cancer. *Drugs* **1994**, *48*, 794–847.
- (4) Trivedi, M.; Budihardjo, I.; Loureiro, K.; Reid, T. R.; Ma, J. D. Epothilones: a novel class of microtubule-stabilizing drugs for the treatment of cancer. *Future Oncol.* **2008**, *4*, 483–500.
- (5) Robinson, H. M. Vinca revisited—another happenstance in the discovery of vinblastine. *Biochem. Cell Biol.* **1991**, *69*, 581–582.

- (6) Griggs, J.; Metcalfe, J. C.; Hesketh, R. Targeting tumour vasculature: the development of combretastatin A4. *Lancet Oncol.* **2001**, *2*, 82–87.
- (7) Rowinsky, E. K.; Donehower, R. C. The clinical pharmacology and use of antimicrotubule agents in cancer chemotherapeutics. *Pharmacol. Ther.* **1991**, *52*, 35–84.
- (8) Attard, G.; Greystoke, A.; Kaye, S.; De Bono, J. Update on tubulin-binding agents. *Pathol. Biol. (Paris)* **2006**, *54*, 72–84.
- (9) Checchi, P. M.; Nettles, J. H.; Zhou, J.; Snyder, J. P.; Joshi, H. C. Microtubule-interacting drugs for cancer treatment. *Trends Pharmacol. Sci.* **2003**, *24*, 361–365.
- (10) Sridhare, M.; Macapinlac, M. J.; Goel, S.; Verdier-Pinard, D.; Fojo, T.; Rothenberg, M.; Colevas, D. The clinical development of new mitotic inhibitors that stabilize the microtubule. *Anti-Cancer Drugs* **2004**, *15*, 553–555.
- (11) Islam, M. N.; Song, Y.; Iskander, M. N. Investigation of structural requirements of anticancer activity at the paclitaxel/tubulin binding site using CoMFA and CoMSIA. *J. Mol. Graphics Modell.* **2003**, *21*, 263–272.
- (12) Pettit, G. R.; Singh, S. B.; Hamel, E.; Lin, C. M.; Alberts, D. S.; Garcia-Kendall, D. Isolation and structure of the strong cell growth and tubulin inhibitor combretastatin A-4. *Experientia* **1989**, *45*, 209–211.
- (13) Young, S. L.; Chaplin, D. J. Combretastatin A4 phosphate: background and current clinical status. *Expert Opin. Invest. Drugs* **2004**, *13*, 1171–1182.
- (14) Delmonte, A.; Sessa, C. AVE8062: a new combretastatin derivative vascular disrupting agent. *Expert Opin. Invest. Drugs* **2009**, *18*, 1541–1548.
- (15) Anderson, H. L.; Yap, J. T.; Miller, M. P.; Robbins, A.; Jones, T.; Price, P. M. Assessment of pharmacodynamic vascular response in a phase I trial of combretastatin A4 phosphate. *J. Clin. Oncol.* **2003**, *21*, 2823–2830.
- (16) Patterson, D. M.; Rustin, G. J. Vascular damaging agents. *Clin. Oncol. (R. Coll. Radiol.)* **2007**, *19*, 443–456.
- (17) Simoni, D.; Romagnoli, R.; Baruchello, R.; Rondanin, R.; Rizzi, M.; Pavani, M. G.; Alloatti, D.; Giannini, G.; Marcellini, M.; Riccioni, T.; Castorina, M.; Guglielmi, M. B.; Bucci, F.; Carminati, P.; Pisano, C. Novel combretastatin analogues endowed with antitumor activity. *J. Med. Chem.* **2006**, *49*, 3143–3152.
- (18) Stevenson, J. P.; Rosen, M.; Sun, W.; Gallagher, M.; Haller, D. G.; Vaughn, D.; Giantonio, B.; Zimmer, R.; Petros, W. P.; Stratford, M.; Chaplin, D.; Young, S. L.; Schnall, M.; O'Dwyer, P. J. Phase I trial of the antivascular agent combretastatin A4 phosphate on a 5-day schedule to patients with cancer: magnetic resonance imaging evidence for altered tumor blood flow. *J. Clin. Oncol.* **2003**, *21*, 4428–4438.
- (19) Aprile, S.; Del Grosso, E.; Tron, G. C.; Grosa, G. In vitro metabolism study of combretastatin A-4 in rat and human liver microsomes. *Drug Metab. Dispos.* **2007**, *35*, 2252–2261.
- (20) Pettit, G. R.; Toki, B.; Herald, D. L.; Verdier-Pinard, P.; Boyd, M. R.; Hamel, E.; Pettit, R. K. Antineoplastic agents. 379. Synthesis of phenstatin phosphate. *J. Med. Chem.* **1998**, *41*, 1688–1695.
- (21) La Regina, G.; Sarkar, T.; Bai, R.; Edler, M. C.; Saletti, R.; Coluccia, A.; Piscitelli, F.; Minelli, L.; Gatti, V.; Mazzoccoli, C.; Palermo, V.; Mazzoni, C.; Falcone, C.; Scovassi, A. I.; Giansanti, V.; Campiglia, P.; Porta, A.; Maresca, B.; Hamel, E.; Brancale, A.; Novellino, E.; Silvestri, R. New arylthioindoles and related bioisosteres at the sulfur bridging group. 4. Synthesis, tubulin polymerization, cell growth inhibition, and molecular modeling studies. *J. Med. Chem.* **2009**, *52*, 7512–7527.
- (22) Tron, G. C.; Pirali, T.; Sorba, G.; Pagliai, F.; Busacca, S.; Genazzani, A. A. Medicinal chemistry of combretastatin A4: present and future directions. *J. Med. Chem.* **2006**, *49*, 3033–3044.
- (23) Gwaltney, S. L.; Imade, H. M.; Barr, K. J.; Li, Q.; Gehrke, L.; Credo, R. B.; Warner, R. B.; Lee, J. Y.; Kovar, P.; Wang, J.; Nukkala, M. A.; Zielinski, N. A.; Frost, D.; Ng, S. C.; Sham, H. L. Novel sulfonate analogues of combretastatin A-4: potent antimetabolic agents. *Bioorg. Med. Chem. Lett.* **2001**, *11*, 871–874.
- (24) Deschesnes, R. G.; Patenaude, A.; Rousseau, J. L.; Fortin, J. S.; Ricard, C.; Cote, M.-F.; Huot, J.; C.-Gaudreault, R.; Petitclerc, E. Microtubule-destabilizing agents induce focal adhesion structure disorganization and anoikis in cancer cells. *J. Pharmacol. Exp. Ther.* **2007**, *320*, 853–864.
- (25) Petitclerc, E.; Deschesnes, R. G.; Cote, M.-F.; Marquis, C.; Janvier, R.; Lacroix, J.; Miot-Noirault, E.; Legault, J.; Mounetou, E.; Madelmont, J.-C.; C.-Gaudreault, R. Antiangiogenic and antitumoral activity of phenyl-3-(2-chloroethyl)ureas: a class of soft alkylating agents disrupting microtubules that are unaffected by cell adhesion-mediated drug resistance. *Cancer Res.* **2004**, *64*, 4654–4663.
- (26) Mounetou, E.; Legault, J.; Lacroix, J.; C.-Gaudreault, R. Antimitotic antitumor agents: synthesis, structure–activity relationships, and biological characterization of *N*-aryl-*N'*-(2-chloroethyl)ureas as new selective alkylating agents. *J. Med. Chem.* **2001**, *44*, 694–702.
- (27) Mounetou, E.; Legault, J.; Lacroix, J.; C.-Gaudreault, R. A new generation of *N*-aryl-*N'*-(1-alkyl-2-chloroethyl)ureas as microtubule disrupters: synthesis, antiproliferative activity, and β -tubulin alkylation kinetics. *J. Med. Chem.* **2003**, *46*, 5055–5063.
- (28) Poyet, P.; Ritchot, N.; Bechard, P.; C.-Gaudreault, R. Effect of an aryl chloroethyl urea on tubulin and vimentin syntheses in a human breast cancer cell line. *Anticancer Res.* **1993**, *13*, 1447–1452.
- (29) Fortin, S.; Moreau, E.; Patenaude, A.; Desjardins, M.; Lacroix, J.; Rousseau, J. L.; C.-Gaudreault, R. *N*-Phenyl-*N'*-(2-chloroethyl)ureas (CEU) as potential antineoplastic agents. Part 2: Role of ω -hydroxyl group in the covalent binding to β -tubulin. *Bioorg. Med. Chem.* **2007**, *15*, 1430–1438.
- (30) Moreau, E.; Fortin, S.; Desjardins, M.; Rousseau, J. L.; Petitclerc, E.; C.-Gaudreault, R. Optimized *N*-phenyl-*N'*-(2-chloroethyl)ureas as potential antineoplastic agents: synthesis and growth inhibition activity. *Bioorg. Med. Chem.* **2005**, *13*, 6703–6712.
- (31) Moreau, E.; Fortin, S.; Lacroix, J.; Patenaude, A.; Rousseau, J. L.; C.-Gaudreault, R. *N*-Phenyl-*N'*-(2-chloroethyl)ureas (CEUs) as potential antineoplastic agents. Part 3: role of carbonyl groups in the covalent binding to the colchicine-binding site. *Bioorg. Med. Chem.* **2008**, *16*, 1206–1217.
- (32) Azim, E.-M.; Dupuy, J.-M.; Maurizis, J.-C.; C.-Gaudreault, R.; Veyre, A.; Madelmont, J.-C. Synthesis of 4-*tert*-butyl-3-(2-chloro- $[-^{14}\text{C}]$ ethyl)ureido benzene. *J. Labelled Compd. Radiopharm.* **1997**, *39*, 559–566.
- (33) Maurizis, J. C.; Rapp, M.; Azim, E. M.; C.-Gaudreault, R.; Veyre, A.; Madelmont, J.-C. Disposition and metabolism of a novel antineoplastic agent, 4-*tert*-butyl-[3-(2-chloroethyl)ureido]benzene, in mice. *Drug Metab. Dispos.* **1998**, *26*, 146–151.
- (34) Fortin, J. S.; Cote, M.-F.; Lacroix, J.; Desjardins, M.; Petitclerc, E.; C.-Gaudreault, R. Selective alkylation of β _{II}-tubulin and thioredoxin-1 by structurally related subsets of aryl chloroethylureas leading to either anti-microtubules or redox modulating agents. *Bioorg. Med. Chem.* **2008**, *16*, 7277–7290.
- (35) Fortin, J. S.; Cote, M.-F.; Lacroix, J.; Patenaude, A.; Petitclerc, E.; C.-Gaudreault, R. Cycloalkyl-substituted aryl chloroethylureas inhibiting cell cycle progression in G₀/G₁ phase and thioredoxin-1 nuclear translocation. *Bioorg. Med. Chem. Lett.* **2008**, *18*, 3526–3531.
- (36) Fortin, J. S.; Cote, M.-F.; Lacroix, J.; Petitclerc, E.; C.-Gaudreault, R. Aromatic 2-chloroethyl urea derivatives and bioisosteres. Part 2: Cytotoxic activity and effects on the nuclear translocation of thioredoxin-1, and the cell cycle progression. *Bioorg. Med. Chem.* **2008**, *16*, 7477–7488.
- (37) Bouchon, B.; Papon, J.; Communal, Y.; Madelmont, J.-C.; Degoul, F. Alkylation of prohibitin by cyclohexylphenyl-chloroethyl urea on an aspartyl residue is associated with cell cycle G₁ arrest in B16 cells. *Br. J. Pharmacol.* **2007**, *152*, 449–455.
- (38) Patenaude, A.; Deschesnes, R. G.; Rousseau, J. L.; Petitclerc, E.; Lacroix, J.; Cote, M.-F.; C.-Gaudreault, R. New soft alkylating agents with enhanced cytotoxicity against cancer cells resistant to chemotherapeutics and hypoxia. *Cancer Res.* **2007**, *67*, 2306–2316.
- (39) Fortin, S.; Labrie, P.; Moreau, E.; Wei, L.; Kotra, L. P.; C.-Gaudreault, R. A comparative molecular field and comparative molecular similarity indices analyses (CoMFA and CoMSIA) of *N*-phenyl-*N'*-(2-chloroethyl)ureas targeting the colchicine-binding site as anticancer agents. *Bioorg. Med. Chem.* **2008**, *16*, 1914–1926.
- (40) Fortin, S.; Wei, L.; Moreau, E.; Labrie, P.; Petitclerc, E.; Kotra, L. P.; C.-Gaudreault, R. Mechanism of action of *N*-phenyl-*N'*-(2-chloroethyl)ureas

in the colchicine-binding site at the interface between α - and β -tubulin. *Bioorg. Med. Chem.* **2009**, *17*, 3690–3697.

(41) Fortin, S.; Moreau, E.; Lacroix, J.; Teulade, J. C.; Patenaude, A.; C.-Gaudreault, R. *N*-Phenyl-*N'*-(2-chloroethyl)urea analogues of combretastatin A-4: Is the *N*-phenyl-*N'*-(2-chloroethyl)urea pharmacophore mimicking the trimethoxy phenyl moiety? *Bioorg. Med. Chem. Lett.* **2007**, *17*, 2000–2004.

(42) Fortin, J. S.; Lacroix, J.; Desjardins, M.; Patenaude, A.; Petitclerc, E.; C.-Gaudreault, R. Alkylation potency and protein specificity of aromatic urea derivatives and bioisosteres as potential irreversible antagonists of the colchicine-binding site. *Bioorg. Med. Chem.* **2007**, *15*, 4456–4469.

(43) Parmee, E. R.; Naylor, E. M.; Perkins, L.; Colandrea, V. J.; Ok, H. O.; Candelore, M. R.; Cascieri, M. A.; Deng, L.; Feeney, W. P.; Forrest, M. J.; Hom, G. J.; MacIntyre, D. E.; Miller, R. R.; Stearns, R. A.; Strader, C. D.; Tota, L.; Wyratt, M. J.; Fisher, M. H.; Weber, A. E. Human β_3 adrenergic receptor agonists containing cyclic ureidobenzene-sulfonamides. *Bioorg. Med. Chem. Lett.* **1999**, *9*, 749–754.

(44) Anthony, N. J.; Lim, J. J.; Su, D.-S.; Wood, M. R. Arylsulfonamide Derivatives. Patent WO/2005/004810, 2005; Merck & Co., Inc.

(45) National Cancer Institute (NCI/NIH), Developmental Therapeutics Program Human Tumor Cell Line Screen. <http://dtp.nci.nih.gov/branches/btb/ivclsp.html> (accessed February 2, 2011).

(46) Fortin, S.; Lacroix, J.; Côté, M.-F.; Moreau, E.; Petitclerc, E.; C.-Gaudreault, R. Quick and simple detection technique to assess the binding of antimicrotubule agents to the colchicine-binding site. *Biol. Proced. Online* **2010**, *12*, 113–117.

(47) Schibler, M. J.; Cabral, F. Taxol-dependent mutants of Chinese hamster ovary cells with alterations in α - and β -tubulin. *J. Cell Biol.* **1986**, *102*, 1522–1531.

(48) Cabral, F.; Sobel, M. E.; Gottesman, M. M. CHO mutants resistant to colchicine, colcemid or griseofulvin have an altered β -tubulin. *Cell* **1980**, *20*, 29–36.

(49) Beck, W. T.; Mueller, T. J.; Tanzer, L. R. Altered surface membrane glycoproteins in Vinca alkaloid-resistant human leukemic lymphoblasts. *Cancer Res.* **1979**, *39*, 2070–2076.

(50) Hu, X. F.; Martin, T. J.; Bell, D. R.; de Luise, M.; Zalberg, J. R. Combined use of cyclosporin A and verapamil in modulating multidrug resistance in human leukemia cell lines. *Cancer Res.* **1990**, *50*, 2953–2957.

(51) Levy, M.; Spino, M.; Read, S. E. Colchicine: a state-of-the-art review. *Pharmacotherapy* **1991**, *11*, 196–211.

(52) Jain, A. N. Morphological similarity: a 3D molecular similarity method correlated with protein-ligand recognition. *J. Comput.-Aided Mol. Des.* **2000**, *14*, 199–213.

(53) Struski, S.; Cornillet-Lefebvre, P.; Doco-Fenzy, M.; Dufer, J.; Ulrich, E.; Masson, L.; Michel, N.; Gruson, N.; Potron, G. Cytogenetic characterization of chromosomal rearrangement in a human vinblastine-resistant CEM cell line: use of comparative genomic hybridization and fluorescence in situ hybridization. *Cancer Genet. Cytogenet.* **2002**, *132*, 51–54.

(54) Ueda, K.; Cardarelli, C.; Gottesman, M. M.; Pastan, I. Expression of a full-length cDNA for the human “MDR1” gene confers resistance to colchicine, doxorubicin, and vinblastine. *Proc. Natl. Acad. Sci. U.S.A.* **1987**, *84*, 3004–3008.

(55) Desbene, S.; Giorgi-Renault, S. Drugs that inhibit tubulin polymerization: the particular case of podophyllotoxin and analogues. *Curr. Med. Chem.: Anti-Cancer Agents* **2002**, *2*, 71–90.

(56) Mooberry, S. L. Mechanism of action of 2-methoxyestradiol: new developments. *Drug Resist. Updates* **2003**, *6*, 355–361.

(57) Verenich, S.; Gerck, P. M. Therapeutic promises of 2-methoxyestradiol and its drug disposition challenges. *Mol. Pharmaceutics* **2010**, *7*, 2030–2039.

(58) Petitclerc, E.; Boutaud, A.; Prestayko, A.; Xu, J.; Sado, Y.; Ninomiya, Y.; Sarras, M. P., Jr.; Hudson, B. G.; Brooks, P. C. New functions for non-collagenous domains of human collagen type IV. Novel integrin ligands inhibiting angiogenesis and tumor growth in vivo. *J. Biol. Chem.* **2000**, *275*, 8051–8061.

(59) Kim, J.; Yu, W.; Kovalski, K.; Ossowski, L. Requirement for specific proteases in cancer cell intravasation as revealed by a novel semiquantitative PCR-based assay. *Cell* **1998**, *94*, 353–362.

(60) Uchibayashi, T.; Lee, S. W.; Kunimi, K.; Ohkawa, M.; Endo, Y.; Noguchi, M.; Sasaki, T. Studies of effects of anticancer agents in combination with/without hyperthermia on metastasized human bladder cancer cells in chick embryos using the polymerase chain reaction technique. *Cancer Chemother. Pharmacol.* **1994**, *35* (Suppl.), S84–S87.

(61) Brooks, P. C.; Silletti, S.; von Schalscha, T. L.; Friedlander, M.; Cheresch, D. A. Disruption of angiogenesis by PEX, a noncatalytic metalloproteinase fragment with integrin binding activity. *Cell* **1998**, *92*, 391–400.

(62) Laemmli, U. K. Cleavage of structural proteins during the assembly of the head of bacteriophage T4. *Nature* **1970**, *227*, 680–685.

(63) Lyu, M. A.; Choi, Y. K.; Park, B. N.; Kim, B. J.; Park, I. K.; Hyun, B. H.; Kook, Y. H. Over-expression of urokinase receptor in human epidermoid-carcinoma cell line (HEp3) increases tumorigenicity on chorio-allantoic membrane and in severe-combined-immunodeficient mice. *Int. J. Cancer* **1998**, *77*, 257–263.

(64) SYBYL, version 8.1; Tripos International (1699 South Hanley Rd, St. Louis, MO, 63144, U.S.).